BEAM CODING
WITH SPREAD SPECTRUM
ORTHOGONAL GOLD CODES
IN UNDERWATER ACOUSTIC SYSTEMS

A THESIS SUBMITTED TO

THE GRADUATE SCHOOL OF ENGINEERING AND SCIENCE

OF BILKENT UNIVERSITY

IN PARTIAL FULFILLMENT OF THE REQUIREMENTS FOR

THE DEGREE OF

MASTER OF SCIENCE

IN

ELECTRICAL AND ELECTRONICS ENGINEERING

By

Andaç BEDER

October, 2015

We certify that we have read this thesis and that in our opinion it is fully adequate, in scope and in quality, as a thesis for the degree of Master of Science.

_____

Prof. Dr. Hayrettin Köymen (Advisor)

_____

Prof. Dr. Ayhan Altıntaş

_____

Asst. Prof. Satılmış Topçu

_____

Dr. Tarık Reyhan

_____

Asst. Prof. Arif Sanlı Ergün

Approved for the Graduate School of Engineering and Science:

_____

Prof. Dr. Levent Onural

Director of the Graduate School

ABSTRACT

BEAM CODING WITH SPREAD SPECTRUM ORTHOGONAL GOLD CODES IN UNDERWATER ACOUSTIC SYSTEMS

Andaç BEDER

M.S in Electrical and Electronics Engineering

Supervisor: Prof. Dr. Hayrettin Köymen

October, 2015

In this study, the applicability of beam coding approaches enabling coded transmission with direct sequence spread spectrum (DSSS) signals to multiple high resolution beams in underwater acoustic systems is investigated. Performance of (DSSS) signals for beam coding application is theoretically analyzed and experimentally proved. Instead of conventional (DSSS) parameters maximal length sequence and binary phase shift keying (BPSK) modulation, gold code sequences are more appropriate for multi-user applications due to their better cross-correlation function and minimum shift keying (MSK) modulation is more appropriate for constant amplitude signals due to its phase continuity. Beam coding experiments were carried out with 511 gold chips sequences with Minimum Shift Keying (MSK) modulation to spread over the frequency range of 70 - 90 kHz. The results of these experiments indicate that each coded signal can be separately detectable after signal processing in Matlab. And this shows that the beam coding approach is implementable in underwater acoustic systems.

Keywords: Beam Coding, Direct Sequence Spread Spectrum, Gold Code Sequence, Minimum Shift Keying.

ÖZET

SUALTI AKUSTİK SİSTEMLERDE YAYILI İZGE TEKNİĞİNİ KULLANARAK ORTOGONAL GOLD KODLAR İLE HUZME KODLAMA

Andaç BEDER

Elektrik Elektronik Mühendisliği, Yüksek Lisans

Tez Yöneticisi: Prof. Dr. Hayrettin Köymen

Ekim, 2015

Bu çalışmada, kodlu Doğrudan Dizili Yayılı İzge (DDYİ) sinyallerinin yüksek çözünürlüklü huzmelerden yayımı ile huzme kodlama yaklaşımının sualtı akustik sistemler için uygulanabilirliği incelenmektedir. Huzme kodlama uygulaması için DDYİ sinyallerinin başarımı teorik açıdan analiz edilmekte ve deneysel yöntemle doğrulanmaktadır. Klasik DDYİ sinyallerinde kullanılan maksimal uzunluk dizileri ve ikili faz kaydırmalı anahtarlama modülasyonu yerine daha iyi çapraz korelasyon fonksiyonuna sahip olduğu için çoklu kullanım uygulamalarına daha uygun Gold kod dizileri ve faz devamlılığına sahip sabit genlikli sinyaller için daha uygun minimum kaydırmalı anahtarlama modülasyonu kullanılmaktadır. Huzme kodlama deneyleri 511'lik Gold kod dizileri 70 – 90 kHz frekans bandına yayılan minimum kaydırmalı anahtarlama modülasyonu yapılarak gerçekleştirilmiştir. Deneylerin sonucu kodlu sinyallerine Matlab programı ile sinyal işleme uygulandıktan sonra kodlu sinyallerin ayrı ayrı tespit edilebildiğini göstermektedir. Bu da huzme kodlama yaklaşımının sualtı akustik sistemler için uygulanabilir olduğunu göstermektedir.

Anahtar sözcükler: Huzme Kodlama, Doğrudan Dizili Yayılı İzge, Gold Kod Dizileri, Minimum Kaydırmalı Anahtarlama.

Acknowledgements

Contents

List of Figures

Chapter 1

1. INTRODUCTION

Underwater acoustic ranging systems are called sonar systems as an abbreviated form for Sound Navigation And Ranging. The principle of most sonar systems is the detection of underwater acoustic waves. Unlike electromagnetic waves, the movement of acoustic waves is provided by mechanical vibrations in its propagation medium such as water [1]. Generation and reception of acoustic wave are carried out by electro acoustic antennas that convert electrical energy to acoustical energy or vice versa [2].

Sonar systems are divided into two common categories, which are passive sonar systems and active sonar systems. Passive sonar systems listen to the underwater environment only without sending any acoustic waves through the water. In active sonar systems, a transmitter antenna called a transducer sends acoustic waves to the surveillance region and a receiver antenna called a hydrophone receives reflected acoustic waves. The active sonar system concept will be used in this study, since coded acoustic signals will be transmitted, received and processed. The purpose is the transmission of coded signals to

different surveillance regions known as "beam coding" for multiple target detection and surveillance region enlargement.

Surveillance regions are called "beam" according to the radiation pattern of the transducers. Single element transducers provide omni directional transmission, which means radiation acoustic waves propagate uniformly all in a direction. Thus, beam coding application with single element transducers is not possible. It is necessary to use a transducer with high directivity, meaning a very narrow main beam to meet the requirement of the beam coding approach. Beam coding is the transmission of distinct coded signals to different beams thanks to the beam steering process. According to one or more coded signals reflected back from the targets, multiple target detections and locating are possible by help of travel time and steering angle information of the coded signals.

Coded signals can be generated by using spread spectrum modulation. This modulation enables the suppressing of the detrimental effects of interference, low probability of intercept and achieving message privacy. In addition to these advantages, spread spectrum modulation also allows for simultaneously multiple coded transmissions by sharing a common channel due to using orthogonal pseudorandom code sequences, which is known as code division multiple-access (CDMA). The beam coding approach shows the same characteristics with those of code division multiple access, since multiple coded sonar signals are simultaneously insonified to distinct beams called by different code sequences. This is known as multiple access phenomena. The beam coding application will be carried out by using the (CDMA) property of spread spectrum.

Some researches were conducted about spread spectrum modulation for underwater acoustic systems. In [3], direct sequence spread spectrum (DSSS) signals were used experimentally to carry out low power range estimation in underwater acoustic by using binary phase shift keying (BPSK) modulation and maximal-length sequence for pseudorandom code sequence. In [4], (DSSS) signals were also used theoretically to carry out covertness and environment friendliness in sonar systems by using binary phase keying (BPSK) modulation

2

and maximal-length sequence for pseudorandom code sequence. In [5, 6], frequency hopped spread spectrum signals were used theoretically to carry out a beam coding in underwater acoustic systems. In this study, (DSSS) signals will be used to carry out a beam coding application by using minimum shift keying (MSK) modulation with gold code sequences for coded beams.

This study consists of six main chapters and these are introduction, beam coding with spread spectrum modulation, pseudorandom code sequence design, alternative modulation technique for (DSSS), beam coding experiment and conclusion. In chapter 2, the means of beam coding application and information about spread spectrum modulation are discussed. In chapter 3, generation and selection of pseudorandom code sequence for (DSSS) signals are discussed. In chapter 4, the advantage of alternative modulation technique (MSK) for (DSSS) signals is analyzed. In chapter 5, the beam coding lake experiment results are shared and discussed in detail. Finally, conclusions obtained from the study are elucidated.

Chapter 2

2. BEAM CODING WITH SPREAD SPECTRUM MODULATION

2.1 Introduction

Conventional modulation techniques of digital communication such as (AM), (PSK) and (FSK) have two major concerns: efficient uses of channel bandwidth and transmit power. However, in some situations, there are more significant requirements, such as covert and secure communication rather than the efficient use of channel bandwidth and transmit power. Spread spectrum modulation means the transmitted signal occupies a bandwidth much wider than the message signal bandwidth by use of pseudorandom codes. This modulation allows many users to share the same bandwidth, multipath (ISI) rejection, mitigation of jamming effects by hostiles and low probability of intercept by eavesdroppers. There are some conventional modulation techniques that occupy a bandwidth much wider than the message signal bandwidth such as frequency modulation types. However, these modulations are not accepted as spread spectrum

modulation. The reason for this is that they do not use pseudorandom codes in order to increase channel bandwidth of transmission.

Besides covert and secure communication, spread spectrum also provides resistance to the inter symbol interference (ISI) stemming from multi-path propagation [7] and multiple-access communication, in which several independent users share a common channel without an external synchronization mechanism [8]. Coded beams are not totally mutually orthogonal; hence beam coding approach benefits from resistance to the inter symbol interference property of the spread spectrum. Multiple coded signals are insonified simultaneously to multiple beams with their distinct specific code sequences; hence beam coding approach also benefits from multiple access phenomena of the spread spectrum.

Spread spectrum modulation based on the kind of spreading modulation is broadly categorized as

- Direct sequence spread spectrum (DSSS) modulation

- Frequency hopping spread spectrum (FHSS) modulation

- Time hopping spread spectrum (THSS) modulation

- Hybrid spread spectrum modulation

The beam coding approach, the main subject of the current thesis, is carried out by using resistance to (ISI) and multiple-access communication properties of spread spectrum modulation and applying direct sequence spread spectrum (DSSS).

2.2 History of Spread Spectrum

The use of bandwidth was much wider than the information bandwidth in the early 1930s without the use of pseudorandom code sequences [9]. The use of real spread spectrum modulation with pseudorandom code sequences came with World War

2. Both the allies and axis countries conducted simple spread spectrum modulation experiments. The first spread spectrum idea for secure communication to guide torpedoes was suggested by Fritz Mandl who was conducting research in weapons control systems for Hitler. However, the first patent on spread spectrum modulation was secured by Hendy Lamarr, the ex-wife of Fritz Mandl, and George Antheil, a music composer, on 11th August 1942 [10]. They did not make any financial profit from this patent, as the patent details were a military secret for many years. Most of the research about spread spectrum modulation was conducted during the 1950s, 1960s and 1970s under military secrecy.

The first commercial use of spread spectrum modulation was applied with direct sequence spread spectrum for multiple access communications in the 1980s. Now, the global positioning system (GPS) is the world's single largest system in which spread spectrum modulation is used [9] [10].

2.3 Notion of Direct Sequence Spread Spectrum Modulation

Direct Sequence Spread Spectrum (DSSS) modulation is one of the spread spectrum techniques in which transmission band spreading is achieved by multiplication of information signal and a binary pseudorandom code sequence whose chip rate is many times higher than the information signal rate. Multiplication of two uncorrelated signals generates a signal whose frequency spectrum is the convolution of these two uncorrelated signals frequency spectrums [11]. Thus, the (DSSS) signal frequency spectrum is nearly the spectrum of the binary pseudorandom sequence. At the receiver side, received signal is multiplied by exactly the same binary pseudorandom sequences. This process is called de-spreading. In this study, the de-spreading process is applied

by matched filter under the assumption of Gaussian random underwater noise. The block diagram of a (DSSS) modulation system is described in Figure 2.1.
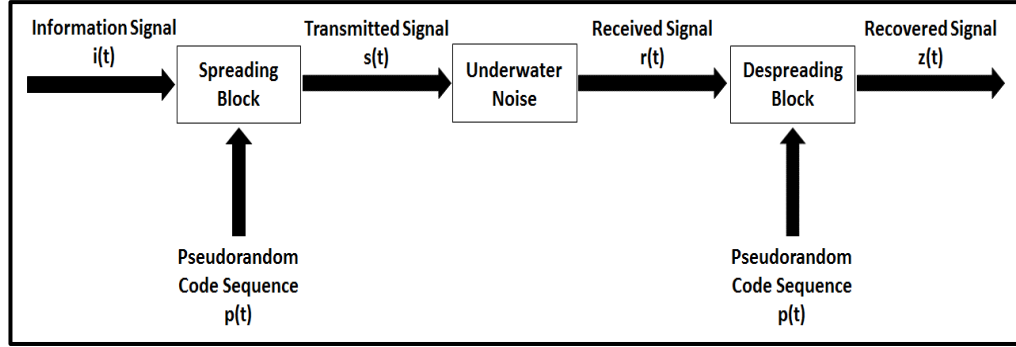
Figure 2.1: Basic (DSSS) System Block Diagram

Information signal can be only a carrier modulated signal and expressed as:

$$i(t) = \cos(2\pi f_c t + \theta)$$

Pseudorandom code sequence can be expressed as:

$$p(t) = \sum_{i=1}^{N} P_A \times rect \left(\frac{t - iT_c}{T_c}\right)$$

where N is pseudorandom code sequence length and P_A determines the amplitude of rectangular function either +1 or -1 in accordance with the rule of pseudorandom code sequence length. T_C is time duration of each bit of code sequence; thus the duration of pseudorandom code sequence is NT_C.

The transmitted signal is the carrier modulated direct sequence spread spectrum signal. It can be expressed as:

$$s(t) = i(t) \times p(t)$$

The received signal consists of attenuated (DSSS) signal and environmental noise can be expressed as:

7

$$r(t) = i(t) \times p\,(t) + n(t)$$

The recovered signal consists of de-spreading information signal and spreading environment noise can be expressed as:

$$z(t) = [i(t) \times p\,(t) + n(t)] \times p\,(t)$$

$$z(t) = i(t) + n_s(t)$$

where $n_s(t)$ is spread environmental noise whose power is spread over a wide frequency band. A small fraction of environmental noise that depends on processing gain can interfere with information signal.

Processing gain is the most crucial advantage of (DSSS) modulation as regards the non-spread spectrum modulations. In a (DSSS) signal, the binary pseudorandom sequence rate is called the chip rate and is denoted by W. The reciprocal of W is called the chip duration and is denoted by T_c. The information signal bit rate is denoted by R. The reciprocal of R is called the information signal duration and is denoted by T_b. The band spreading factor can be expressed as:

$$B_e = \frac{W}{R} = \frac{T_b}{T_c}$$

where $\dfrac{W}{R}$ an integer is the ratio of (PN) code sequence bandwidth to the information bandwidth that is also called the processing gain.

2.4 Beam Coding with Direct Sequence Spread Spectrum Modulation

The response of electro-acoustic antennas can vary according to direction which is called a beam pattern of antennas [12]. These spatial variations depend on the operational frequency, shape and size of electro-acoustic antennas. A beam pattern of the antenna can consist of the main beam, side lobes and grating lobes.

The main beam characterized by an aperture of -3 dB at maximum is called a "beam" in this study.

Some signal parameters such as transmission frequency and signal duration determine the individual characteristics of acoustic signals. However, these parameters are not adequate in transmitting different acoustic signals to distinct beams due to the operational requirements and limitation of electro-acoustic antenna. Acoustic signals can be modulated with independent code sequences and transmitted to distinct beams, which is called "beam coding".

The performance improvement obtained from a (DSSS) signal is thanks to the processing gain. Processing gain enables the sharing of the same channel bandwidth with many (DSSS) signals. (DSSS) signals are separable from each other by means of their own pseudorandom code sequence. This capability provides simultaneous transmission of more than one (DSSS) signal over the same channel bandwidth. Each (DSSS) signal can be orientated to different beams by electronic beam steering. Beam steering changes the direction of the acoustic wave to a specific location by altering the relative phase of array elements. As a result, distinct (DSSS) signals are simultaneously assigned to each beam.

The beam can be formed in any direction via the electrically appropriate amount delaying the signal to each element of transducer array, which is called beam steering. Active sonar systems can apply beam steering by using conventional acoustic signals in order to cover the whole coverage area. However, there is a need for round trip times so as to cover the whole coverage area for monostatic systems. During these round trip times, the array must not be steered otherwise some targets are missed. This round trip time which is related with maximum detection range (R_m) and velocity of sound (c) is equal to $2R_m/c$. There is also a need for (β/α) acoustic signals to complete the whole coverage area where β is the surveillance region coverage area angle and α is the beamwidth angle. Hence, the time to cover the complete coverage area is equal to $2R_m/c \times \beta/\alpha$. For instance, an active sonar system has a maximum range of 1.5 km and has a surveillance region coverage area angle of 15° with a 1.5°

beamwidth. The time to cover the complete coverage area will be $2x1500/1500\ x\ 15/1.5\ =\ 20$ seconds. This delay is significantly high in an active sonar system if the target is moving. Regardless of the round trip delay of beam steering, beam coding is recommended so as to scan the whole coverage area simultaneously.

By using the beam coding application, the coverage area of an active sonar system can be increased without the need for more channel bandwidth or time. Beam coding with (DSSS) signals can be applicable as illustrated in Figure 2.2.
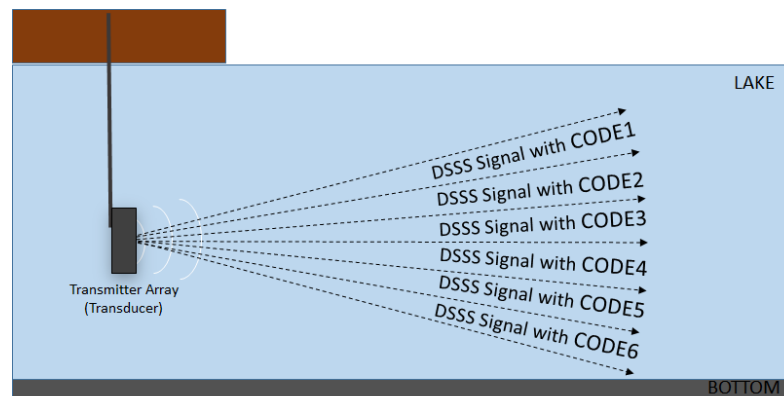
Figure 2.2: Beam Coding with (DSSS) Signals

In Figure 2.2, 6 different beams are coded with 6 distinct (DSSS) signals. The number of coded beams might change in accordance with the operational requirements. However, each (DSSS) signal appears as additive interference for other (DSSS) signals. The level of interference depends on mutual orthogonality (PN) code sequences and the number of coded beams. There is a need to determine the usable maximum number of coded beams in accordance with orthogonality of (PN) code sequences, since (PN) code sequences are not totally orthogonal in practice, even if it is assumed that they are mutually orthogonal. The selection of good mutual orthogonal (PN) code sequences, which is a crucial problem for beam coding application, will be discussed in the following chapter.

Chapter 3

3. PSEUDORANDOM (PN) CODE SEQUENCE DESIGN

3.1 Introduction

The generation of pseudorandom (PN) code sequence is fundamental in direct sequence spread spectrum (DSSS) applications, as (DSSS) technique consists of multiplying the input data by a (PN) code sequence whose bit rate is much higher than the input bit rate. The result is wideband and noise like waveform.

     (PN) sequences are deterministic and periodic, not totally random. The generation of (PN) code sequence is performed by the outputs of linear feedback shift register systems. The linear feedback shift register system consists of consecutive two-state memory blocks (shift registers) and feedback logic blocks (exclusive OR logic). The m-stage linear shift register system is illustrated in Figure 3.1. Binary sequences in memory are shifted through the next shift registers. The new binary content of the first register is determined by a logical combination of some other shift registers.
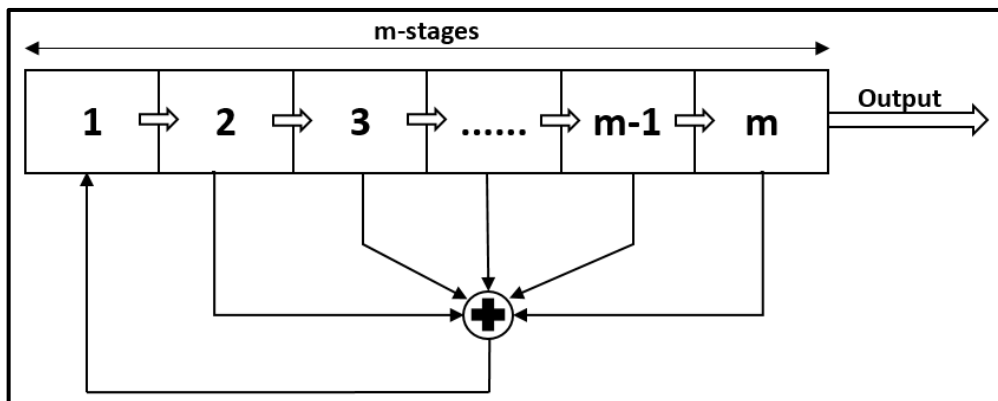
Figure 3.1: m- stage linear shift register system

For multiple user applications of the (DSSS) technique, the cross-correlation and autocorrelation properties of the (PN) sequence are significant. Each user should be assigned a particular (PN) sequence that should be mutually orthogonal with other (PN) sequences to reduce the level of interference among users. However, some level of interference among (PN) sequences is experienced in practice. Thus, the autocorrelation function of (PN) sequence should have a relatively high peak. That is, the peak-off value of the autocorrelation function should be much smaller than the peak value of the autocorrelation function. The cross-correlation function of (PN) sequences should be relatively small, ideally zero.

In the (DSSS) applications, the binary polar sequence elements {'0' and '1'} are mapped onto corresponding bipolar sequences elements {'-1' and '1'}. Because the multiplication of the input data with a pseudorandom code sequence, the '0' element results in energy loss in the input data. Therefore, it is bipolar sequences that are applied, rather than polar elements.

In this section, the generation of maximal length sequences and gold sequences will be briefly explained while also discussing their cross-correlation and autocorrelation properties.

3.2 Maximal Length Sequences

The most common (PN) sequences are the maximal length sequences (m-sequence) for (DSSS) applications. M-sequences are the largest code sequences that can be generated by a linear shift register system. The m-sequence includes $m=2^n-1$ codes where "n" is the number of shift registers in the linear shift register system.

The linear shift register system function G(D) for m-sequences generation has to be a primitive polynomial. The primitive polynomials are special polynomials that are not the products of any lower degree two polynomials. The primitive polynomials also divide D^M+1 in module-2 domain. The reciprocal polynomial of any primitive polynomial is also a primitive polynomial. The reciprocal polynomial of G(D) is

$$G_r(D) = D^n.G(1/D)$$

The number of distinct m-sequences depends only on the number of distinct primitive polynomials for any linear shift register system. The number of primitive polynomials of degree "n" where "n" is the number of shift register is equal to

$$N_p = \frac{2^n-1}{n} \prod_{i=1}^{k} \frac{P_i-1}{P_i}$$

where P_i {i=1, 2, ……. k} is the prime factor of $2^n - 1$.

For instance, in an n=3 linear shift register system, the prime factor of $2^3 - 1$ is only 7. Thus, the number of primitive polynomials of such a system is

$$N_p = \left(\frac{2^3-1}{3}\right)\left(\frac{7-1}{7}\right) = 2$$

The primitive polynomials of such a system are as follows:

$D^7+1 = (D+1). (D^3+D+1).(D^3+D^2+1)$ in module-2 domain.

Primitive polynomials: $G_1(D) = (D^3+D^2+1)$ and $G_2(D) = (D^3+D+1)$

There are 2 primitive polynomials for a linear shift register system that consists of 3 shift registers. It can also be easily calculated to indicate that $G_1(D)$ is a reciprocal polynomial of $G_2(D)$ or vice versa.

$G_{2r}(D) = D^3 (D^{-3} +D^{-1}+1)$

$G_{2r}(D) = 1+ D^2 + D^3 = G_1(D)$

The generation of m-sequence code process for $G_1(D)$ and $G_2(D)$ is illustrated in Figure 3.2.

In Figure 3.2, the initial states of shift registers are '1' '1' and '1'. Each linear shift register system whose function is a primitive polynomial can generate only one m-sequence code, regardless of the initial state of shift registers. The generation of m-sequence code process is cyclic, as the initial state change of shift registers results in generating phase shifted replica of either of the originals.

For a more complex linear shift register system, it is difficult to find primitive polynomials. The tables of primitive polynomials have been generated for quick reference. The tables of primitive polynomials may be found in [16] [17].
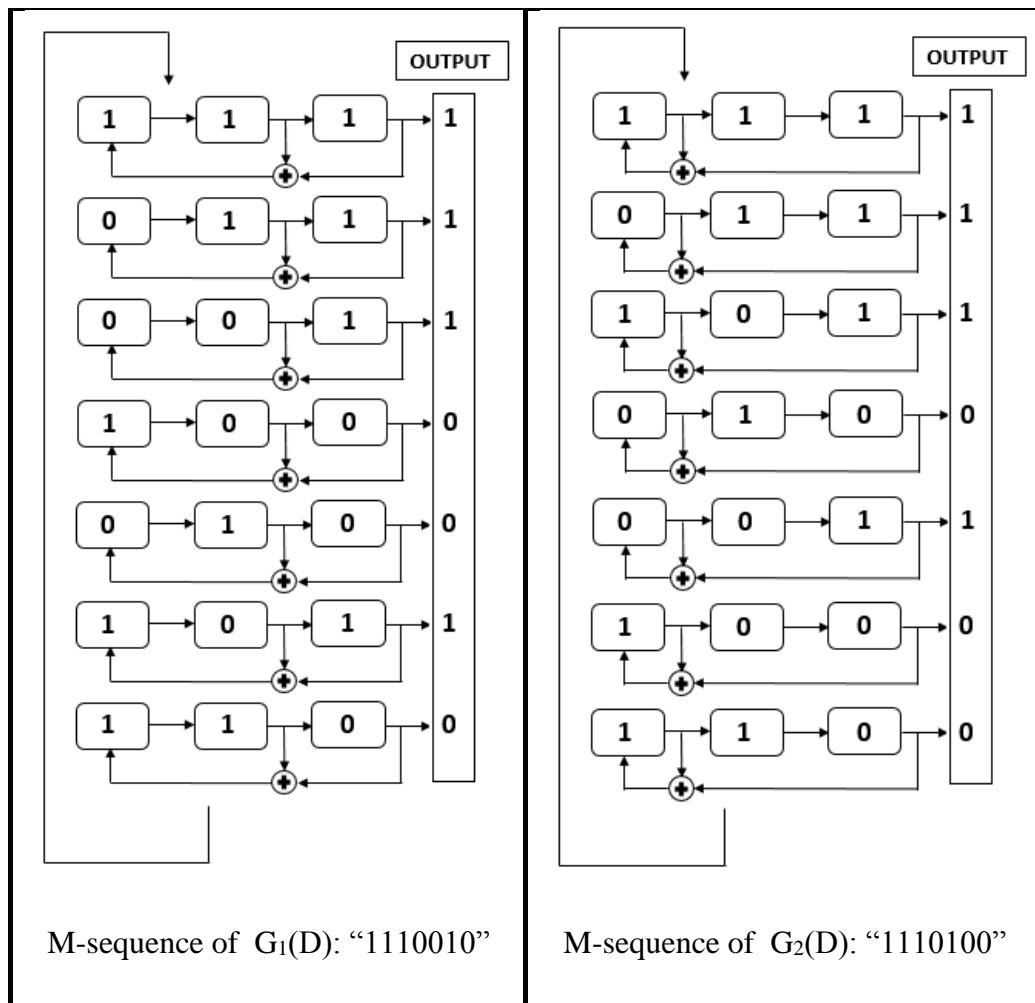
Figure 3.2: Generation of M-sequence Code Process

The striking characteristic of the m-sequence code is its periodic autocorrelation function, due to the periodicity of m-sequences.

In the ideal case, the autocorrelation function of PN sequences is

$$R(j) = \begin{cases} m, & j = 0 \\ 0, & 1 \leq j \leq n - 1 \end{cases}$$

The periodic autocorrelation function of m-sequences is,

$$R(j) = \begin{cases} m, & j = 0 \\ -1, & 1 \leq j \leq n - 1 \end{cases}$$

However, autocorrelation function of long m-sequence is,

$$R(j) = \begin{cases} m, & j = 0 \\ \lim_{m \to \infty} \left(\dfrac{-1}{m} \right) = 0, & 1 \le j \le n - 1 \end{cases}$$

Thus, the m-sequence code becomes an almost ideal sequence in terms of its autocorrelation. In Figure 3.3, the periodic autocorrelation function of an m-sequence consisting of 7 codes is plotted. As expected, the peak value in the plot is 7 and the peak-off value in the plot is only -1. In Figure 3.4, the periodic autocorrelation function of an m-sequence consisting of 511 codes is plotted. As expected, the peak value in the plot is 511. However, the other value seems to be zero, even if the peak-off value in the plot is also -1.
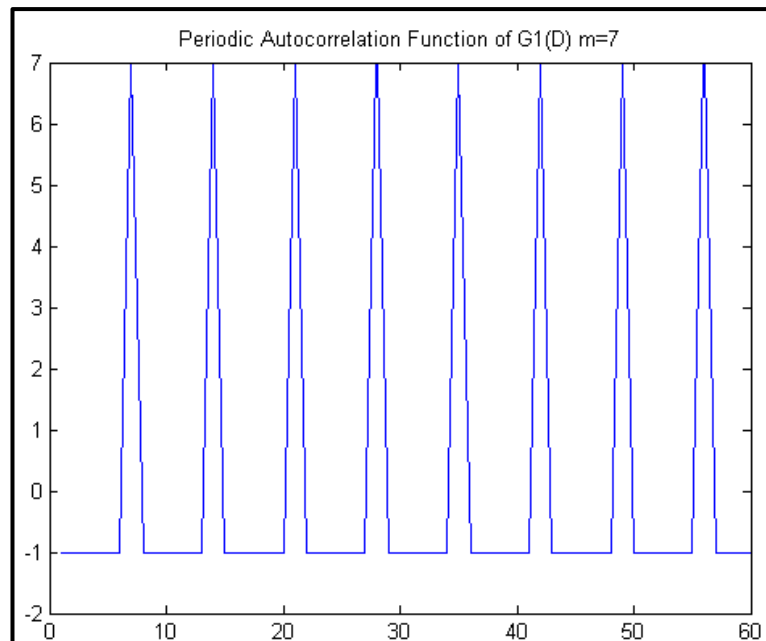
Figure 3.3: The Periodic Autocorrelation Function of M-sequence m=7 codes
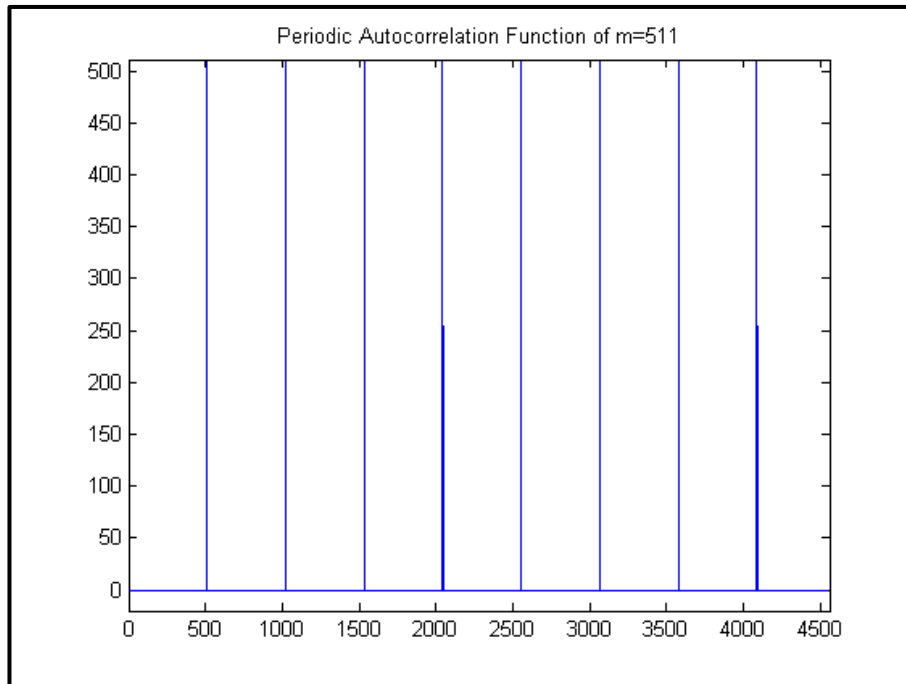
Figure 3.4: The Periodic Autocorrelation Function of M-sequence m=511 codes

For beam coding applications, the cross-correlation characteristic of (PN) sequences are as important as the autocorrelation characteristic of (PN) sequences. This is because each beam is assigned as a particular sequence code that should be ideally mutually orthogonal in order to minimize interference among the beams. The cross-correlation characteristic of m-sequences is also a periodic function. However, the peak-off values of cross-correlation can have relatively large peaks. Hence, m-sequences are not appropriate code sequences for beam coding applications.
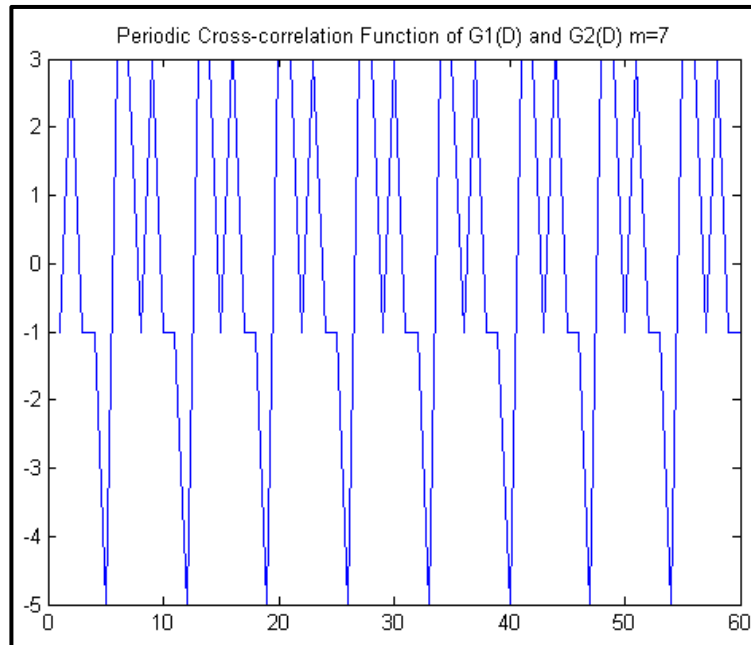
Figure 3.5: Periodic Cross-Correlation Function of G_1(D) and G_2(D):

In Figure 3.5, the periodic cross-correlation function of m-sequences G_1(D) and G_2(D) that consist of 7 codes is plotted. The absolute peak value in the plot is five (5). The peak value of m-sequence cross-correlation function in Figure 3.5 is relatively high with respect to the peak value of m-sequence autocorrelation function: seven (7). This means that, if m-sequence consisting of 7 codes is applied for beam coding, the level of interference can be 71%. The interference percentage relatively decreases by increasing the length of the m-sequence code. However, the interference percentage does not drop below 10% until m = 8191.

3.3 Gold Code Sequences

Gold code sequences have smaller cross-correlation peak values and larger code sequences domains than m-sequences. These two advantages of gold code sequences make more desirable code sequences for beam coding applications.

Gold code sequences are derived from a combination of two specific m-sequences which are called preferred sequences. These two m-sequences of length $m=2^n-1$ indicate periodic cross-correlation functions with three values, which are $\{-1, -t(n), t(n)-2\}$ where;

$$t(n) = \begin{cases} 2^{(n+1)/2} + 1, & odd \; n \\ 2^{(n+2)/2} + 1, & even \; n \end{cases}$$

The generation of gold sequence processes is as follows:

1. Finding a preferred pair of m-sequences of $G_1(D)$ and $G_2(D)$.

2. Taking the sum of $G_2(D)$ and $G_1(D)$ in the module-2 domain or vice versa.

3. Taking the sum of $G_2(D)$ and one code shifted version of $G_1(D)$.

4. Making the same summation until $m=2^n-1$ shifted version of $G_2(D)$.

5. Giving m new periodic sequences.

6. Including original sequences $G_1(D)$ and $G_2(D)$, "m+2" sequences.

These "m+2" sequences are called gold sequences. For instance, m-sequences of $G_1(D)$ and $G_2(D)$ are preferred m-sequences. They were generated in the previous section (Maximal Length Sequence) and were shown in Figure 3.2. The generation of gold code sequences process by using m-sequences of $G_1(D)$ and $G_2(D)$ is illustrated in Figure 3.6.

$G_1(D)$:	1	1	1	0	0	1	0
⊕	⊕	⊕	⊕	⊕	⊕	⊕	⊕
$G_2(D)$:	1	1	1	0	1	0	0
=	=	=	=	=	=	=	=
Gold Code 1:	0	0	0	0	1	1	0

Shift 1 $G_1(D)$:	0	1	1	1	0	0	1
⊕	⊕	⊕	⊕	⊕	⊕	⊕	⊕
$G_2(D)$:	1	1	1	0	1	0	0
=	=	=	=	=	=	=	=
Gold Code 2:	1	0	0	1	1	0	1

Shift 2 $G_1(D)$:	1	0	1	1	1	0	0
⊕	⊕	⊕	⊕	⊕	⊕	⊕	⊕
$G_2(D)$:	1	1	1	0	1	0	0
=	=	=	=	=	=	=	=
Gold Code 3:	0	1	0	1	0	0	0

Shift 3 $G_1(D)$:	0	1	0	1	1	1	0
⊕	⊕	⊕	⊕	⊕	⊕	⊕	⊕
$G_2(D)$:	1	1	1	0	1	0	0
=	=	=	=	=	=	=	=
Gold Code 4:	1	0	1	1	0	1	0

Shift 4 $G_1(D)$:	0	0	1	0	1	1	1
⊕	⊕	⊕	⊕	⊕	⊕	⊕	⊕
$G_2(D)$:	1	1	1	0	1	0	0
=	=	=	=	=	=	=	=
Gold Code 5:	1	1	0	0	0	1	1

Shift 5 $G_1(D)$:	1	0	0	1	0	1	1
⊕	⊕	⊕	⊕	⊕	⊕	⊕	⊕
$G_2(D)$:	1	1	1	0	1	0	0
=	=	=	=	=	=	=	=
Gold Code 6:	0	1	1	1	1	1	1

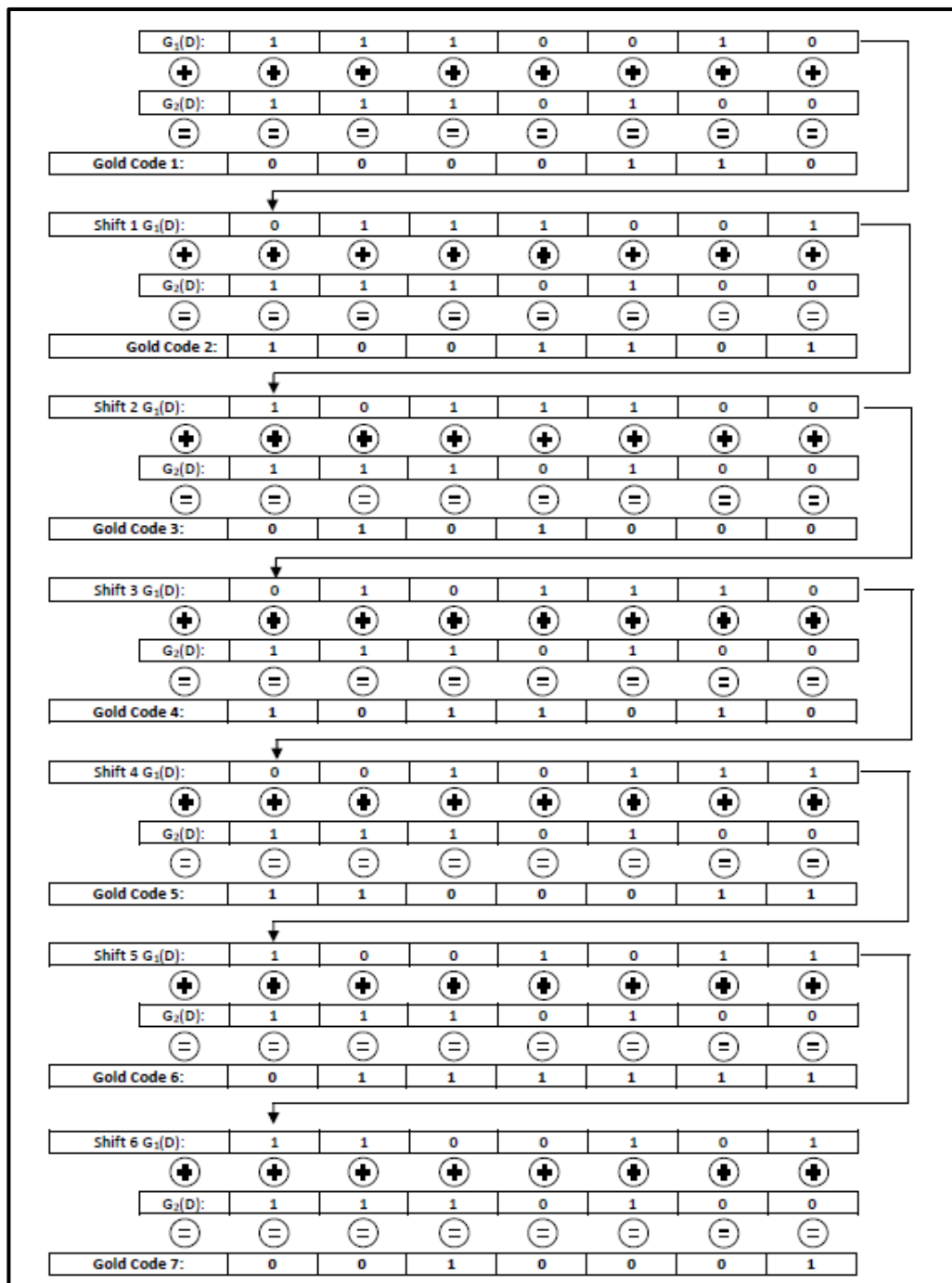| Shift 6 $G_1(D)$:	1	1	0	0	1	0	1
⊕	⊕	⊕	⊕	⊕	⊕	⊕	⊕
$G_2(D)$:	1	1	1	0	1	0	0
=	=	=	=	=	=	=	=
Gold Code 7:	0	0	1	0	0	0	1

Figure 3.6: Generation of Gold Code Sequence Process

According to Figure 3.6, nine gold code sequences containing seven new gold code sequences and two preferred maximal length sequences are generated by using two preferred maximal length sequences where m=7. The set of gold code sequences generated by maximal length sequences $G_1(D)$ and $G_2(D)$ are as follows:

1. Preferred Maximal Length Sequence 1 $G_1(D)$: "1110010"
2. Preferred Maximal Length Sequence 2 $G_2(D)$: "1110100"
3. Gold Code 1: "0000110"
4. Gold Code 2: "1001101"
5. Gold Code 3: "0101000"
6. Gold Code 4: "1011010"
7. Gold Code 5: "1100011"
8. Gold Code 6: "0111111"
9. Gold Code 7: "0010001"

Autocorrelation functions of gold code sequences are also periodic due to the periodicity of gold code. Nonetheless, their autocorrelation functions are not as good as the autocorrelation function of m-sequences; since the peak-off value is not only -1, as seen in Figure 3.7. The peak-off values of gold code 4 are 3 and -5. The peak-off values of gold code 7 are 3 and -1. This autocorrelation function randomness decreases the performance of matched filter at the receiver.

In Figure 3.8, the periodic cross-correlation function of gold code 4 and gold code 7 is plotted. As was explained before, their cross-correlation function consists of -1, -t(n) and t(n)-2 values, where $t(n) = 2^{(3+1)/2} + 1 = 5$.
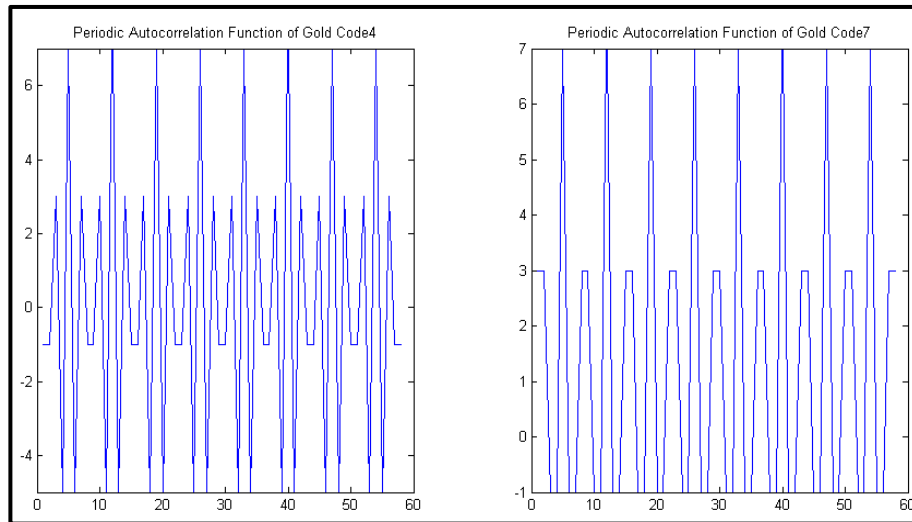
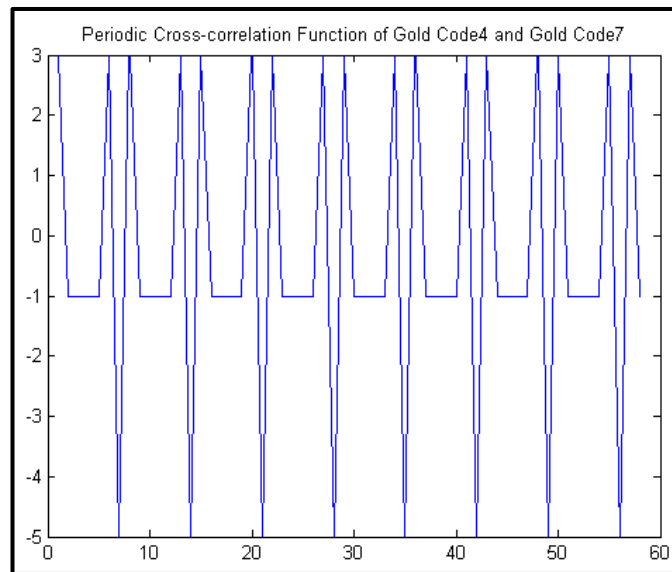Figure 3.7: Periodic Autocorrelation Function of Gold Code4 and Gold Code7

Figure 3.8: Periodic Cross-Correlation Function of Gold Code4 and Gold Code7

The peak value of gold code cross-correlation in Figure 3.8 is the same with the peak value of m-sequence cross-correlation in Figure 3.5. This means that cross-correlation of gold code for m=7 is not better than cross-correlation of m-sequence for m=7. Nevertheless, gold code sequences offer better cross-

correlation properties than m-sequences for longer code sequences. Peak cross-correlation values of m-sequences and gold code sequences are plotted in Figure 3.9 with respect to code length. The peak cross-correlation values of m-sequences decrease slowly by increasing the length of binary code in sequence and the level of inference decreases more than 20% for m=511. On the other hand, the peak cross-correlation values of gold code sequences decrease constantly by increasing the length of binary code in sequence and the level of inference decreases less than 10% for m=511. Thus, gold code sequences are more suitable for beam coding application than m-sequences, especially for long code sequences thanks to better cross-correlation properties and larger number of code sequence sets.
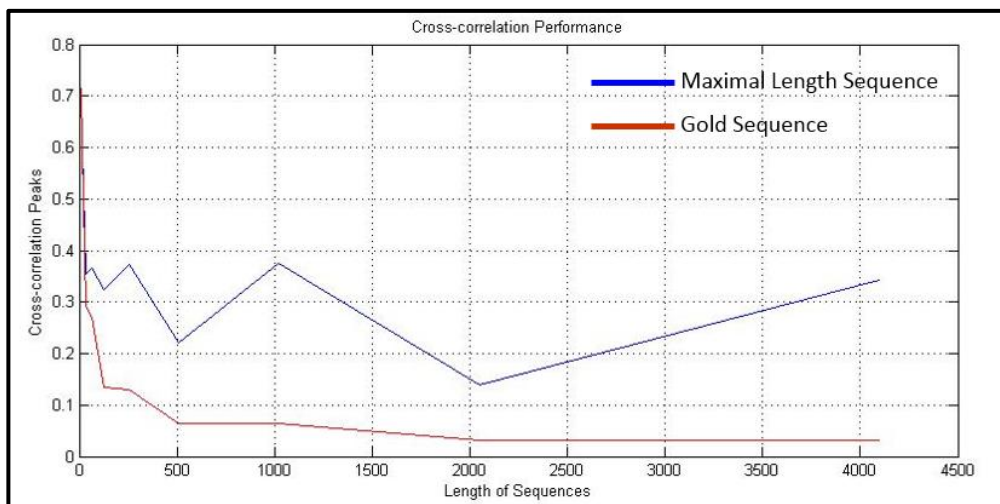

Figure 3.9: Peak Cross-correlation of m-Sequences and Gold Code Sequences

It was previously mentioned that gold code sequences are not totally perfect PN sequences due to their autocorrelation randomness characteristic. For this reason, there arises a need for more research on the generation of PN sequences that have better autocorrelation and cross correlation functions than m-sequences and gold code sequences. In addition to the well-known m-sequences and gold code sequences, the Walsh-Hadamard and Kasami code sequences are also mentioned for direct sequence spread spectrum application in literature.

Chapter 4

4. ALTERNATIVE MODULATION TECHNIQUE FOR PN CODES

4.1 Introduction

Orthogonal (PN) code sequences should be modulated with a type of modulation such as amplitude modulation (AM), phase shift keying (PSK) or frequency shift keying (FSK). (PSK) is more practical in (DSSS) applications in spite of its certain disadvantages. In this chapter, binary phase shift keying (BPSK) in (DSSS) application will be briefly described and its disadvantages will be examined. Then, alternative minimum shift keying (MSK) in (DSSS) applications will be elaborated.

4.2 Conventional DSSS Modulation: Binary Phase Shift Keying (BPSK)

In literature, the most widely known and used modulation technique is Binary Phase Shift Keying (BPSK) modulation for binary case (DSSS) signals. In this modulation, the transmitted information is conveyed by phase of the carrier signal. In (BPSK), binary signals can be represented as follows:

$$s(t) = \cos\big(2\pi f_c t + \pi(m-1)\big) \qquad m = 1, 2 \tag{4.1}$$

$$s(t) = \begin{cases} \cos(2\pi f_c t) & \text{for binary '1'} \\ -\cos(2\pi f_c t) & \text{for binary '0'} \end{cases} \tag{4.2}$$

As can be seen in Equation (4.2), the (BPSK) modulation is straightforward. The binary '1' is represented by the cosines function and the binary '0' is represented by 180° phase shift of the cosines function. Eventually, (BPSK) modulated (DSSS) signal is equivalent to the multiplication of the continuous wave signal and the (PN) binary code sequence. The duration of each code in the (PN) binary code sequence is T, while its amplitude is either 1 or -1 depending on the polarity of the code.

Two different (BPSK) modulated (DSSS) signals are plotted in Figure 4.1 and 4.2. These (BPSK) modulated signals' carrier frequencies f_c are 80 kHz and their chips duration is $T = 12.5$ μs. Therefore, the null-to-null bandwidth of Binary Phase Shift Keying is $\frac{2}{T} = 160\ kHz$.
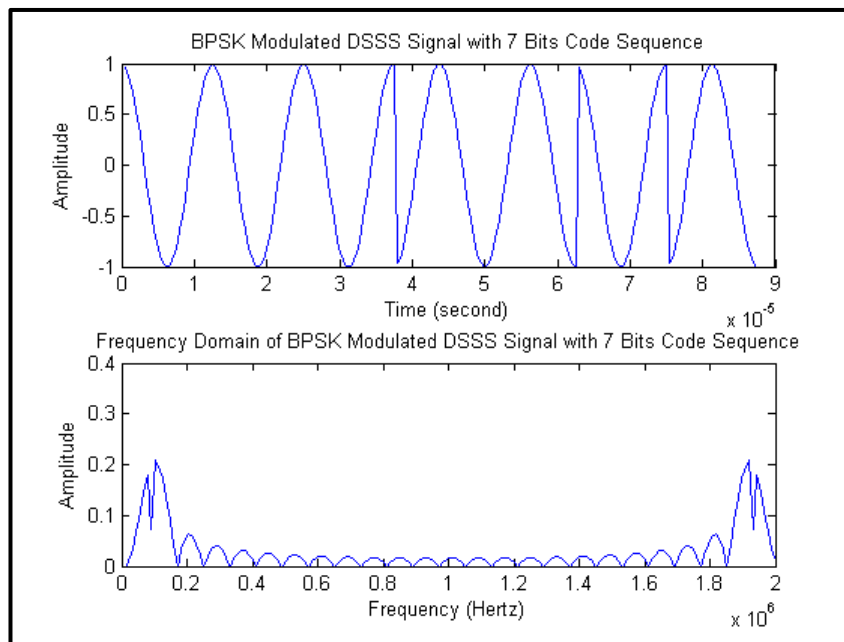
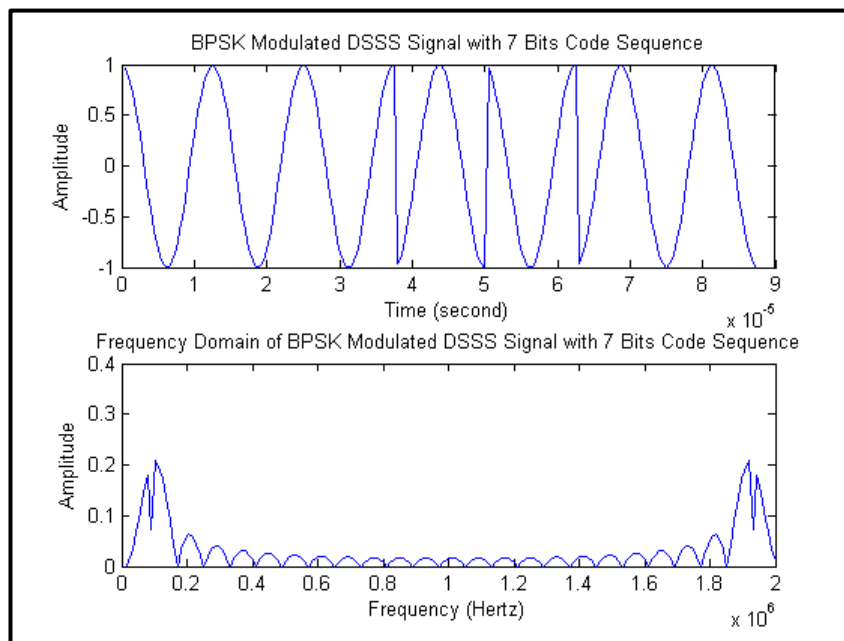Figure 4.1: (MSK) Modulated (DSSS) Signals with Code = [1 1 1 0 0 1 0]

Figure 4.2: (MSK) Modulated (DSSS) Signals with Code = [1 1 1 0 0 1 0]

It is seen in Figure 4.1 and 4.2 that there are jumps in the waveform of (BPSK) modulated (DSSS) signals in time domain. These jumps result in energy of signal scattering out of channel band due to the discontinuity of phase. Because of the loss of signal energy, the detection performance of receiver side processing is reduced.

Besides the theoretical energy scattering problem of BPSK modulation, using (BPSK) modulated (DSSS) signals leads to an operational problem for an underwater acoustic transducer. This problem is known as "spike problem" due to the phase discontinuity between binary '1' and binary '0' code transition or vice versa. Each phase jumping in waveform generates spike waveforms. These spikes were firstly observed from the measurement of receiver hydrophone data at the Lake Test. The measurement of receiver hydrophone data is plotted in Figure 4.3.
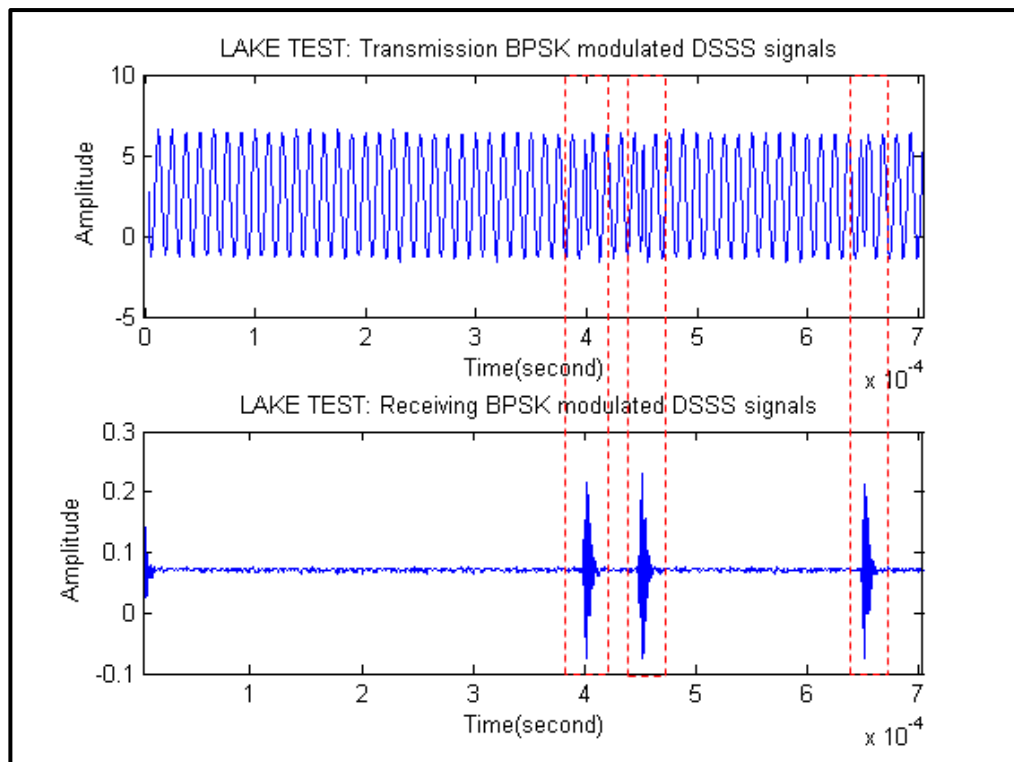

Figure 4.3: Transmitted and Received (BPSK) Modulated (DSSS) Signals at the Lake Test

As seen in Figure 4.3, phase discontinuity can be observed at 0.4, 0.45 and 0.65 ms in the transmitted (BPSK) modulated (DSSS) signal plot. In response to this, there appear spikes at the 0.4, 0.45 and 0.65 ms in the received (BPSK) modulated (DSSS) signal plot. These spikes were observed for all (BPSK) modulated (DSSS) signals at the Lake Test results. The main reason for the appearance of these spikes can be the mechanical capability of the acoustic transducer. The acoustic transducer does not give a real time response as fast as each phase shifting in waveform does.

Alternative modulation techniques such as Gaussian Phase Shift Keying [3] can be suggested for (DSSS) applications in order to prevent the signal energy scattering to other bands and eliminating the spike problem. However, applying Gaussian filter on modulated signal results in non-constant amplitude signal transmission, which reduces the covertness performance of the (DSSS) signal. Thus, continuous phase modulation techniques can be an alternative modulation for (DSSS) signals. These modulations may enable constant amplitude signal transmission, the prevention of the signal energy loss and spike problem.

4.3 Alternative DSSS Modulation: Continuous Phase Frequency Shift Keying (CPFSK)

The conventional modulation is Binary Phase Shift Keying (BPSK) for binary case (DSSS) signals, but (BPSK) modulation has side effects due to phase discontinuity. Hence, Continuous Phase Frequency Shift Keying (CPFSK) modulation can be suggested as an alternative modulation for (DSSS) signals. (CPFSK) signal is generally defined as follows:

$$s(t) = \cos[2\pi f_c t + \theta(t)] \tag{4.3}$$

where $\theta(t)$ is the phase of $s(t)$. The phase of the signal is a continuous function of time by definition of (CPFSK). According to binary code sequence, phase of

signal linearly increases or decreases in the course of the binary code duration. The phase of signal $\theta(t)$ is defined as follows:

$$\theta(t) = \theta(0) \pm \frac{\pi h}{T}t \qquad \text{for } 0 \leq t \leq T \qquad (4.4)$$

where T is the bit duration and h dimensionless parameter is called the deviation ratio. Phase of signal $s(t)$ increases linearly by help of the plus sign, which corresponds to binary code '1', and decreases linearly by the help of the minus sign, which corresponds to binary code '0'. Due to the plus and minus signs in phase definition, binary code '1' and binary code '0' can be represented by different frequencies that are defined as follows:

$$\text{Frequency of Binary Code '1':} \qquad f_1 = f_c + \frac{h}{2T} \qquad (4.5)$$

$$\text{Frequency of Binary Code '0':} \qquad f_2 = f_c - \frac{h}{2T} \qquad (4.6)$$

There are two results of these relations. The first one is the carrier frequency f_c, which is the arithmetic mean of the f_1 and f_2. And the second one is the h deviation ratio which is the difference of the f_1 and f_2 normalized with respect to bit rate [18].

$$\text{The carrier frequency:} \qquad f_c = \frac{1}{2}(f_1 + f_2) \qquad (4.7)$$

$$\text{The deviation ratio:} \qquad h = T(f_1 - f_2) \qquad (4.8)$$

The special case of (CPFSK) is Minimum Shift Keying (MSK) in which the deviation ratio h is assigned to $1/2$. Due to h $= 1/2$ and Equation 4.8, the frequency difference between the frequency of binary code '1' f_1 and frequency of binary code '0' f_2 is $1/2T$. This difference is the minimum frequency separation that is necessary to ensure the orthogonality of signals over bit duration T, since the inner product of two orthogonal signals has to be zero.

$$\text{Re}[< s_1 s_2 >] = Re\left[\int_0^T s_1 s_2^* \, dt \right] = 0 \qquad (4.9)$$

$$Re[< s_1 s_2 >] = Re \left[\int_0^T e^{j2\pi(f_1 - f_2)t} dt \right]$$

$$Re[< s_1 s_2 >] = Re \left[\frac{T \sin(\pi(f_1 - f_2)T)}{\pi(f_1 - f_2)T} e^{j\pi(f_1 - f_2)T} \right]$$

$$Re[< s_1 s_2 >] = T \text{sinc}\big(2T(f_1 - f_2)\big) \qquad (4.10)$$

According to (4.10), if $\text{sinc}\big(2T(f_1 - f_2)\big) = 0$, then s_1 and s_2 are orthogonal signals. This is possible if and only if the frequency difference of s_1 and s_2 signals equals to $k/2T$ in which k is a positive integer. Thus, the minimum frequency separation is $1/2T$ when $k = 1$. This explains why (CPBSK) with h $=$ 1/2 is called (MSK) [8].
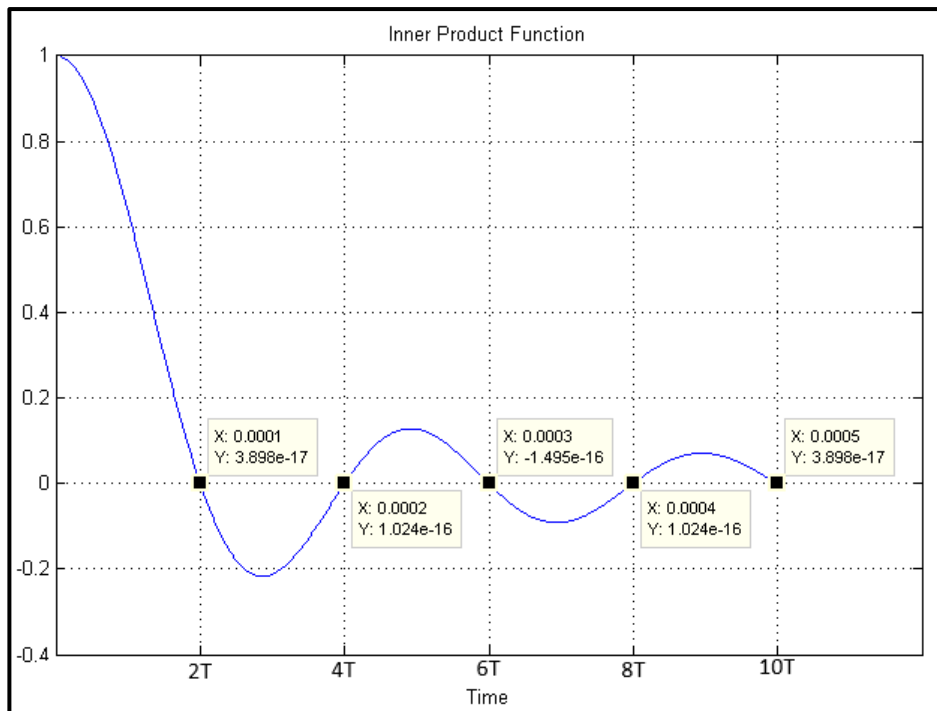

Figure 4.4: Inner Product Plot for T=0.05ms Signals

In order to generate a (MSK) signal $s(t)$, in-phase and quadrature component of the (MSK) signal should be expressed by applying trigonometric identities on Equation (4.3) as follows:

$$s(t) = \cos[\theta(t)]\cos(2\pi f_c t) - \sin[\theta(t)]\sin(2\pi f_c t)$$

In-phase component: $\qquad S_I(t) = \cos[\theta(t)]$

Quadrature component: $\qquad S_Q(t) = \sin[\theta(t)]$

The in-phase and quadrature component can be expressed by using Equation (4.4) as follows:

In-phase component: $\qquad S_I(t) = \cos\left[\theta(0) \pm \frac{\pi}{2T}t\right]$

$$S_I(t) = \cos[\theta(0)]\cos\left(\frac{\pi}{2T}t\right) \pm \sin[\theta(0)]\sin\left[\frac{\pi}{2T}t\right] \qquad (4.11)$$

Quadrature component: $\qquad S_Q(t) = \sin\left[\theta(0) \pm \frac{\pi}{2T}t\right]$

$$S_Q(t) = \cos[\theta(0)]\sin\left[\frac{\pi}{2T}t\right] \pm \sin[\theta(0)]\cos\left(\frac{\pi}{2T}t\right) \qquad (4.12)$$

As was explained before, phase component $\theta(t)$ of a (MSK) signal increases or decreases in terms of the binary value in which phase of (MSK) signal increases $\frac{\pi}{2}$ by binary '1' and decreases $\frac{\pi}{2}$ by binary '0'. The effect of the binary value can also be observed in Equations (4.11) and (4.12). The plus sign in Equation (4.11) corresponds to binary '0' and the minus sign in Equation (4.11) corresponds to binary '1'. On the other hand, the plus sign in Equation (4.12) corresponds to binary '1' and the minus sign in Equation (4.12) corresponds to binary '0' [18]. By the help of these derivations, (MSK) modulated (DSSS) signals are plotted in Figure 4.5 and 4.6. These (MSK) signals carrier frequencies f_c are $20\ kHz$ and their chips duration is $T = 50\ \mu s$. Therefore, the binary '1' code represents $f_1 = 25\ kHz$ and the binary '0' code represents $f_2 = 35\ kHz$. For a linear modulation such as (BPSK,) the null-to-null frequency band spread is $\frac{2}{T} =$

40 kHz. However, the frequency band spreads of (MSK) signals are higher than $\frac{2}{T} = 40\ kHz$ because of the nonlinearity of (MSK) modulation. The null-to-null frequency band spread of MSK signals are approximately 30 kHz in Figure 4.5 and Figure 4.6.

As seen in Figure 4.5 and Figure 4.6, there are no jumps in the waveform of the (MSK) signal due to continuity of phase. This continuity prevents signal energy to spread to other bands which provides a higher signal to noise ratio at the receiver side.
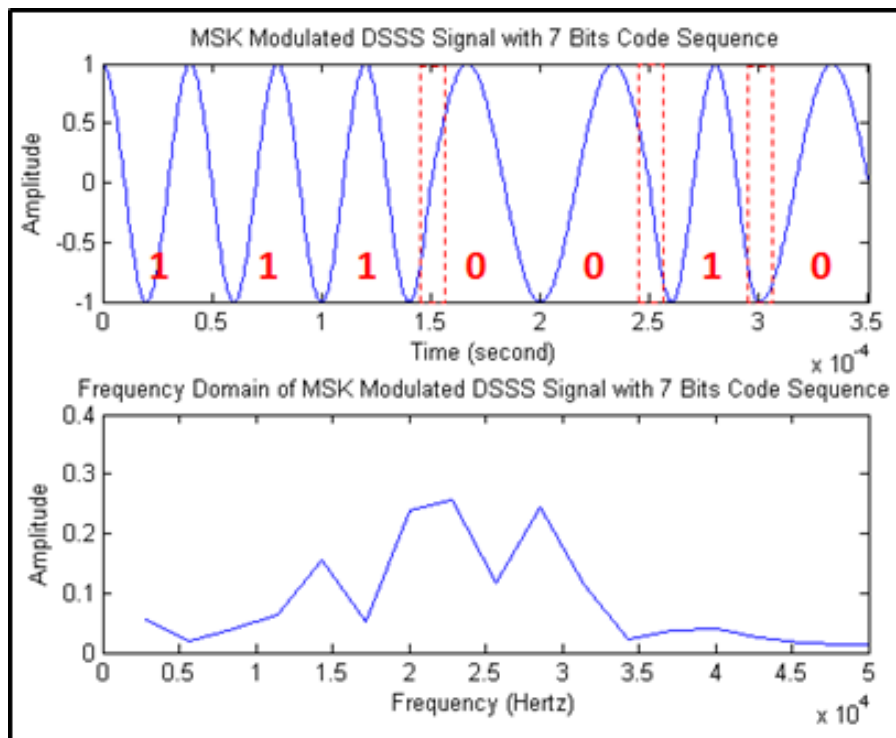

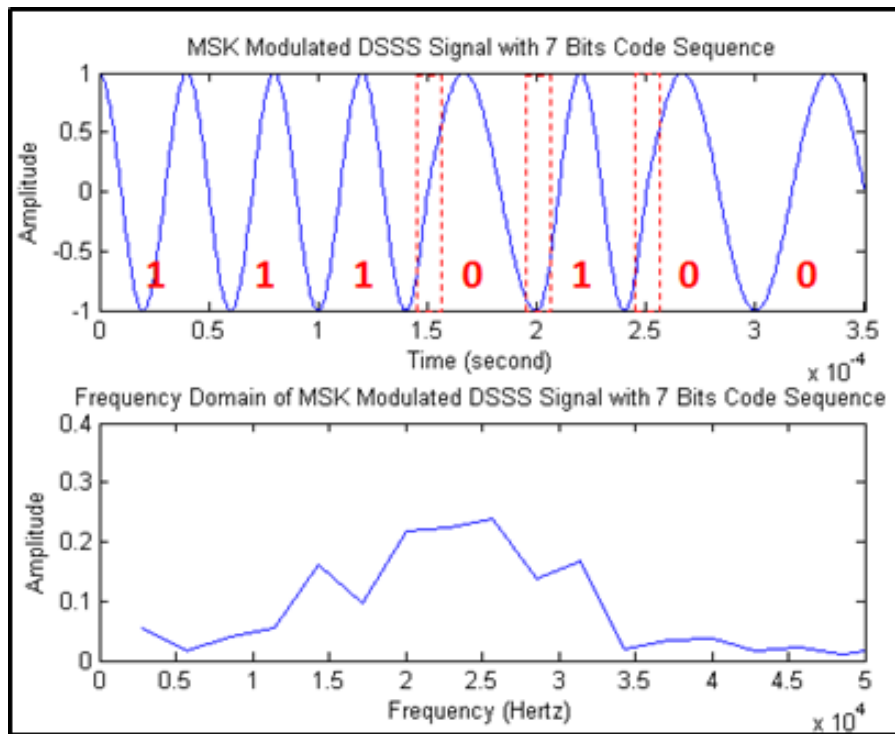Figure 4.5: (MSK) Modulated (DSSS) Signals with Code = [1 1 1 0 0 1 0]

Figure 4.6: (MSK) Modulated (DSSS) Signals with Code = [1 1 1 0 1 0 0]

4.4 The Distortion Problems of Wideband DSSS Acoustic Signals

Wideband DSSS signals' both magnitude and phase response with respect to their frequency range play an important role in the beam coding application, as beam coding benefits from high autocorrelation performance of transmitted and received DSSS signals. Nonlinear magnitude and/or phase response results in distortion on wave shape of DSSS signals. Due to these magnitude and/or phase distortion of DSSS signals, the beam coding performance is reduced. In this study, the attenuation loss problem related to nonlinear magnitude response and the group delay distortion problem related to nonlinear phase response are worked on. However, no equalizer was implemented in order to correct these distortions, since the aim of this study is the proving of the beam coding concept.

33

4.4.1 The Attenuation Loss Problem

Attenuation loss is one effect of a variety of propagation phenomena in the sea. Sea water dissipative propagation medium for acoustic signals converts the acoustic signal energy into heat energy due to effects of absorption, leakage out of channel and scattering. In this study, absorption loss is a significant loss phenomenon, since it strongly depends on the frequency variation of acoustic signals.

Absorption loss (γ) results in the exponential decrease of acoustic signal energy and is expressed in dB unit. Absorption coefficient (α) results in the linear decrease of acoustic signal energy and is expressed in dB/km unit. The relation between absorption coefficient (α) and absorption loss (γ) is as follows [19]:

$$\alpha = 20\gamma \log e \approx 8.686\gamma$$

The absorption of sound in seawater is caused by two factors which are viscosity and ionic relaxation chemical reactions. There are two kinds of viscosity; namely, shear and volume viscosity. Also, there are two kinds of ionic relaxation: magnesium sulfate and boric acid molecules relaxation. The dominant factor of absorption loss is ionic relaxation at the 70-90 kHz frequency band, which is the frequency band of this study. The Fischer-Simmons absorption coefficient expression is as follows [12]:

$$\alpha = A_1 P_1 \left(\frac{f^2}{f_1^2 + f^2} \right) f_1 + A_2 P_2 \left(\frac{f^2}{f_2^2 + f^2} \right) f_2 + A_3 P_3 f^2$$

where A_1, A_2, A_3, f_1 and f_2 are complicated temperature dependent functions. P_1 represents the effects of boric acid with function of pressure. P_2 represents the effects of magnesium sulfate with function of pressure. P_3 represents the effects of viscosity with function of pressure. The simpler form of absorption coefficient expression is as follows [12]:

$$\alpha = \left(\frac{0.1f^2}{1+f^2}\right) + \left(\frac{40f^2}{4100+f^2}\right) + 2.75 \times 10^{-4}f^2 + 0.003$$

The absorption loss increases rapidly with frequency and the order of magnitude is highly variable [19]. At 70 kHz, the absorption loss coefficient will be approximately 23 (dB/kyd) and at 90 kHz, the absorption loss coefficient will be approximately 29 (dB/kyd). This means that the 70 kHz signal components' amplitude will be twice as high as that of the 90 kHz signal components' amplitude in linear scale due to the absorption loss.

In this study, the DSSS signals energy is spread to the 70-90 kHz frequency band. This means that the DSSS signals components are variously affected by the absorption loss. The amplitude of the DSSS signals are distorted due to the absorption loss coefficient high difference between the 70 kHz signal components and the 90 kHz signal components. Hence, the amplitude distortion results in beam coding performance reduction.

The magnitude distortion equalizer can be employed in order to annihilate the absorption loss problem on the DSSS signals for beam coding applications. However, the aim of this study is the proof of the beam coding concept; thus the magnitude distortion equalizer was not employed so as to observe the worst case performance of the beam coding application.

4.4.2 The Group Delay Distortion Problem

Group delay distortion is one effect of a variety of phase responses in the overall underwater acoustic system. Group delay (τ) is defined as the time delay variation on modulated sinusoidal acoustic signal, expressed by phase response differentiating with respect to frequency, and is shown as follows:

$$\tau = \frac{d\,\phi(w)}{dw} = -\frac{1}{2\pi}\frac{d\,\phi(f)}{df}$$

where $\phi(w)$ function of angular frequency (w) is phase response of signal. If the phase response of signal is linear function at operating frequency range, group delay will be constant at operating frequency range. This preserves the modulated acoustic signal wave shape and eliminates the group delay distortion problem.

The distortion of received signal in an underwater acoustic system is caused by any device within the whole system. Hence, the transfer function knowledge of all devices is required in order to diminish group delay distortion. However, it is difficult to determine transfer functions of some devices such as the transfer function of underwater medium. On the other hand, the transfer functions of some devices such as electroacoustic antennas can be measured so as to minimize group delay distortion.

In this study, the phase response of electroacoustic antennas are significant for beam coding that includes various frequency components at the 70-90 kHz frequency band. The phase response transducer and hydrophone are not available. However, it is known that the phase response linearity of electroacoustic antennas are better at off resonance frequencies. In beam coding experiments, electroacoustic antennas were used at off resonance frequencies. Also, the group delay distortion equalizer was not employed so as to observe the worst case performance of the beam coding application; since the aim of this study is the proof of beam coding concept.

Chapter 5

5. THE BEAM CODING EXPERIMENT

5.1 Introduction

The aim of the experiment indicates that beam coding is performed by coded beams by sharing the same bandwidth possible with help of the (DSSS) modulation's multiple access property. To accomplish this aim, several experiments were conducted in Lake Environment. Firstly, a coded (DSSS) signal was transmitted throughout a beam in order to measure the matched filter performance of one coded beam. Secondly, the summation of seven coded (DSSS) signals was transmitted throughout a beam in order to measure interference performance of (DSSS) signals under underwater environmental conditions.

In the previous chapters, we discussed orthogonal code design and the selection of the modulation technique for orthogonal code sequences, which are critical parameters for (DSSS) modulation. In light of these discussions, (DSSS)

signal parameters are decided as 511 chips gold code sequences and (MSK) modulation for beam coding experiments.

In this chapter, the experimental factor of Yalıncak Lake, the experimental setup and the experimental methodology are briefly introduced. The experimental results are shared, visualized and discussed in detail.

5.2 The Experimental Factor of Yalıncak Lake

Beam coding experiments were conducted at Aselsan Inc. underwater acoustic research and measurements of Yalıncak Lake platform which is in the Middle East Technical University Campus. Environmental factors are mostly a crucial part of underwater acoustic experiments. The performance of experiments can degrade because of many different noise sources. For this reason, before beginning the experiments, the noise level of Yalıncak Lake was measured and recorded by hydrophone without any transmission. The noise level of Yalıncak Lake underwater environment is under 2 mV, as illustrated in Figure 5.1.
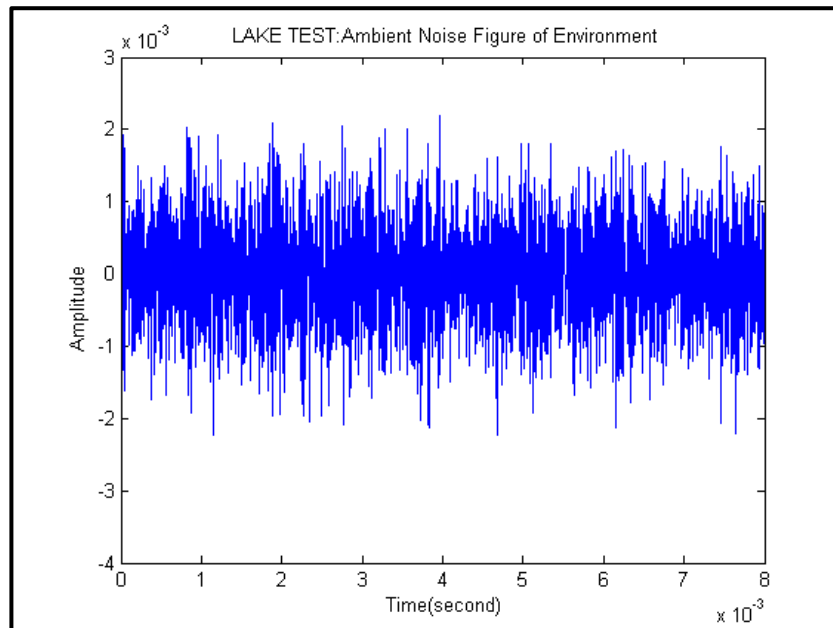

Figure 5.1: Yalıncak Lake Underwater Noise Measurement

Noise sources of underwater environment can be grouped under four categories, which are ambient noise, self-noise, reverberation and acoustic interference [19]. Ambient noise originates from natural and man-made activities such as wind, wave, rain, animals and shipping. These are independent of sonar systems. Self-noise is directly related with acoustic systems that can suffer from their own electronic thermal noise. Reverberation originates from undesired echoes of sonar signal that can mask desired echo of sonar signal. Acoustic interference originates from other acoustic sources in the underwater environment that can interfere with the signal channel.

During the experimental measurements, there was possibly some ambient noise due to natural activities, but there was no man-made ambient noise. Self-noise of acoustic systems (transducer and hydrophone) are also inevitable. Reverberation was observed from received hydrophone data due to multi-path and other reflections. Acoustic interference was not observed by any other acoustic source that interfered with our signal band.

5.3 The Experimental Setup

The experimental setup consists of five electronic devices, which are an arbitrary waveform generator, a power amplifier, a transducer, a hydrophone and oscilloscope and two software programs: Matlab and Agilent Bench-link Waveform Builder.

The arbitrary waveform generator is a 33522A Function and Arbitrary Waveform Generator, 30 MHz by Agilent Technology. The transducer is a D45 omni directional transducer by Neptune Sonar, whose transmitting voltage response (TVR) graph is shown in Appendix A. The hydrophone is a TC4014-5 omni directional hydrophone including pre-amplifier electronics by Teledyne Reson, whose receiving sensitivity graph is shown in Appendix A. The

Oscilloscope is a DPO 7104 Digital Phosphor Oscilloscope by Tektronix. The power amplifier is a Brüel & Kjaer Power Amplifier Type 2713.

In Appendix A, the magnitude response of D45 omni directional transducer and TC4014-5 omni directional hydrophone are given. Besides magnitude response, phase response of electroacoustic antennas is also crucial, especially with the signals that include various frequency components as DSSS signals. Phase response of electroacoustic antennas should be a linear function of frequency and as a consequence, the group delay should be constant at all frequency bands. Linear phase response enables the transmission of various frequencies contained in a modulated waveform to be delayed by the same amount. This provides preventing the signal shape and avoiding phase distortion. The phase response of D45 omni directional transducer and TC4014-5 omni directional hydrophone are not available. Therefore, the phase response of these electroacoustic antennas is assumed on the worst case in the beam coding experiments in order to observe the worst case performance of the DSSS signals.

The experimental setup block diagram starts with (DSSS) signal generation on the Matlab software program. After the generation of the (DSSS) signal, the Agilent Bench-link Waveform Builder software program is used so as to translate Matlab (DSSS) signal coefficients to the appropriate file format for the arbitrary waveform generator. (DSSS) signal is generated by the Arbitrary Waveform Generator block and the amplitude of the signal is amplified 100 times by the power amplifier. The transducer converts the transmitted DSSS electrical signal to acoustic signal and transmits the acoustic signals into the underwater medium. The hydrophone converts the acoustic signal to an electrical signal that is the received (DSSS) signal. Both transmitted and received (DSSS) signals are observed, measured and recorded by the oscilloscope. The recorded data is carried out with several Matlab implementations, which are band pass filtering, matched filtering and peak detection.
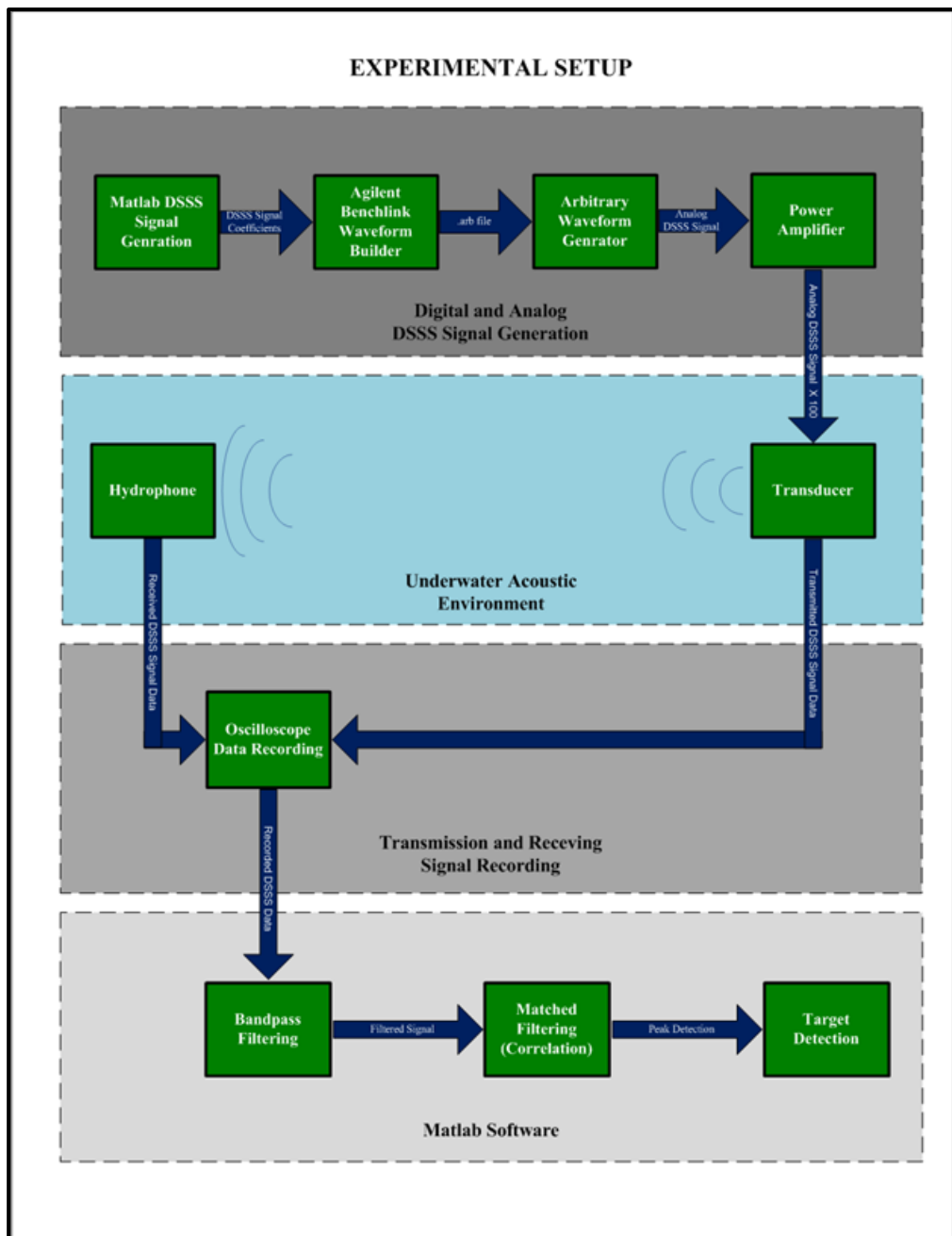
Figure 5.2: Beam Coding Experiment Setup

5.4 The Experimental Result

The time domain and the frequency domain representations of transmitted (DSSS) signals, received (DSSS) signals and matched filter output results are plotted and examined in two steps of the experiment. The first step is related with the measurement of the matched filter performance of one coded (DSSS) signal transmission. The second step is related with measurement interference performance of seven coded (DSSS) signal transmission.

In the first step of the experiment, a 511 chips gold sequence coded (DSSS) signal was transmitted throughout a beam in order to measure the matched filter performance. The time domain and the frequency domain representations of the transmitted (DSSS) signals are plotted in Figure 5.5, in which the signal consists of 511 chips gold code sequence, each chip having 50 μs duration in the sequence. As a result of the transmitted (DSSS) signal, it can be observed that the total duration is 25.55 ms. The carrier frequency of gold code sequence is 80 kHz. Due to the 50 μs chip duration, binary '1' chips are symbolized by 4.25 sinusoidal cycles at 85 kHz and binary '0' chips are symbolized by 3.75 sinusoidal cycles at 75 kHz. The binary '0' chip and the binary '1' chip signal in the transmitted (DSSS) signal is illustrated in Figure 5.3.
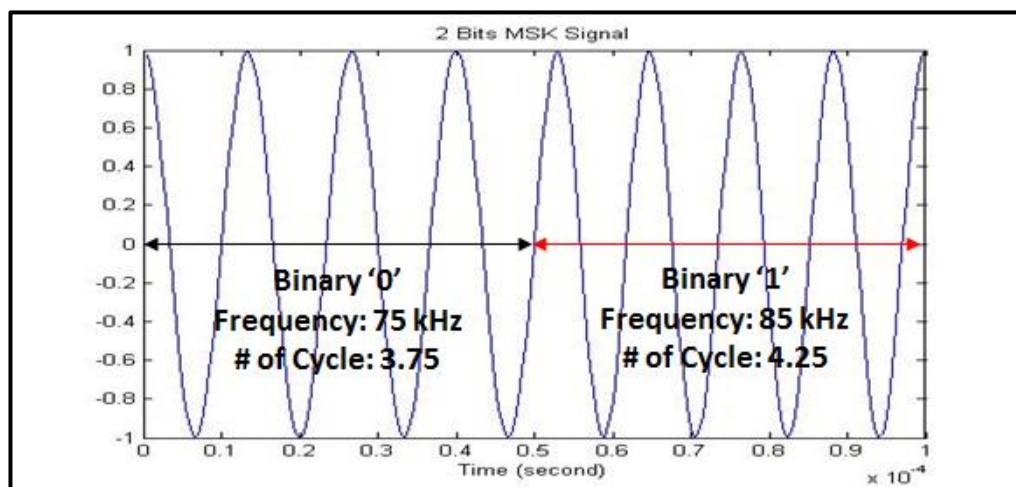

Figure 5.3: Binary '1' and Binary '0' Representation

The time domain and the frequency domain representations of the received (DSSS) signals are plotted in Figure 5.5. Even if the received (DSSS) signal has the same frequency domain characteristic with the transmitted (DSSS) signal, the effect of environmental noise and reverberation is observable on the received signal at the time domain. The received signal duration is longer than the transmitted signal duration: 25.55 ms because of the interference of the desired echo and the undesired surface reflection echo.

The matched filter output result is plotted in Figure 5.7. Matched filter output has 2 peaks that correspond to direct path and surface multi-path of the transmitted (DSSS) signal. The first peak is approximately at 8.35 ms with an estimated range of 12.525 meters and the second peak is approximately at 9.4 ms with an estimated range of 14.1 meters by assumption of 1500 m/s sound velocity. These results are verified by the current experimental setup dimension.
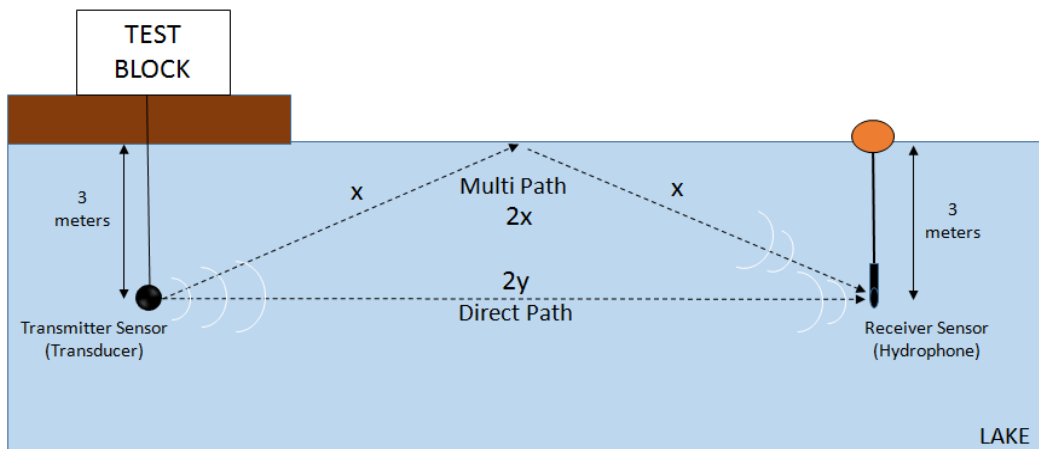

Figure 5.4: Direct Path and Multipath of (DSSS) Signal

It is assumed that the first peak on the matched filter output is the direct path of (DSSS) signal, and then the direct path distance $2y$ is equal to 12.525 meters. The surface multipath distance under the assumption of constant sound velocity profile in underwater environment can be calculated as follows:

$$2x = 2 \times \sqrt[2]{3^2 + \left(\frac{12.525}{2}\right)^2} = 13.888 \, m$$

The expected multipath distance 13.888 m is almost equal to the measured multipath distance 14.1 m. It is also proved that DSSS signals can overcome inter symbol interference by multipath propagation.
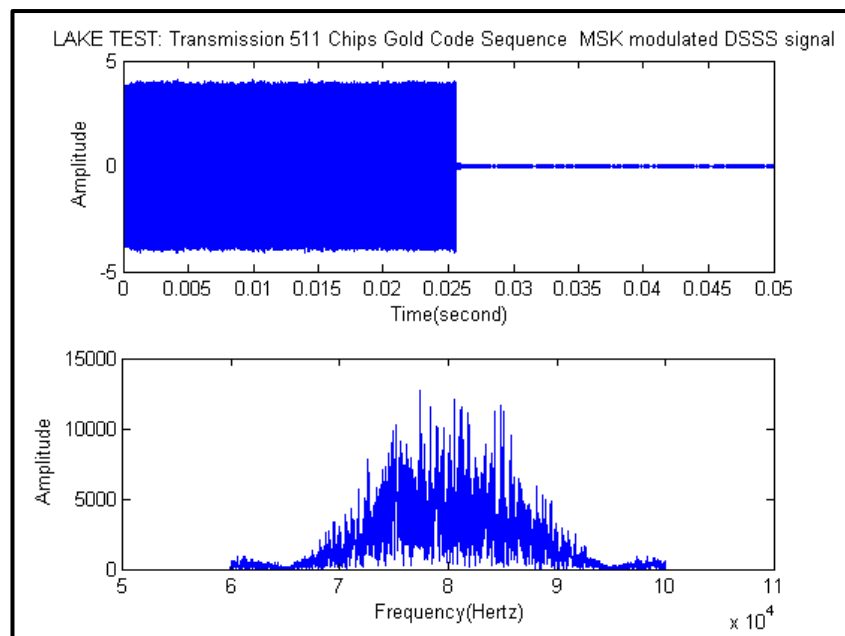

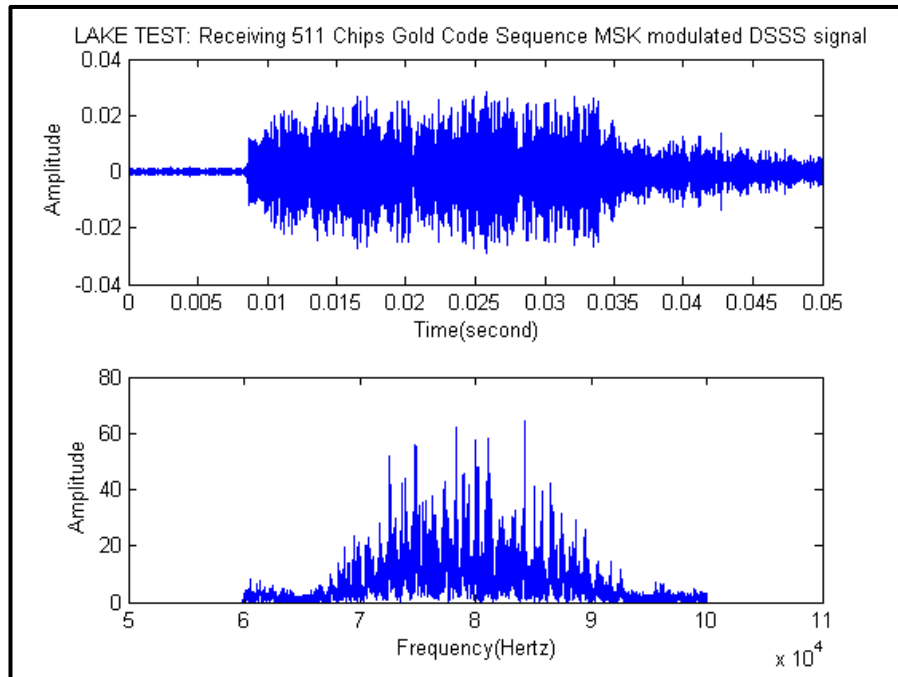Figure 5.5: Time Domain and Frequency Domain Representations of (DSSS) Transmitted Signal

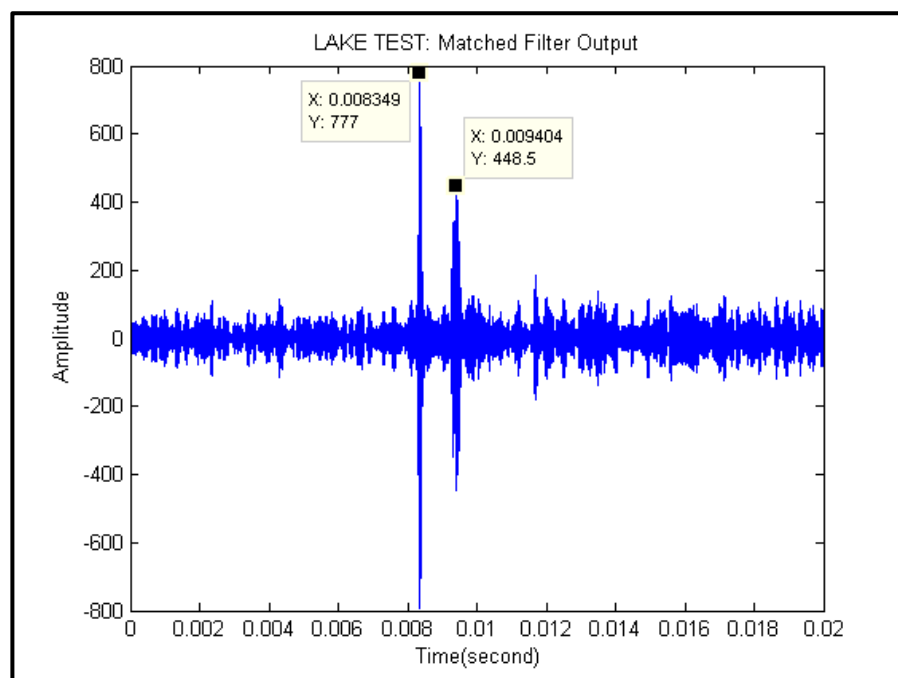Figure 5.6: Time Domain and Frequency Domain Representations of (DSSS) Received Signal

Figure 5.7: The Matched Filter Output

45

In the second step of the experiment, summation of seven 511 chips gold sequence coded (DSSS) signals was transmitted throughout a beam in order to measure the interference performance of (DSSS) signals. The time domain and the frequency domain representations of the transmitted (DSSS) signal are plotted in Figure 5.8, in which the signal consists of summation seven, 511 chips gold code sequence. Each 511 chips gold sequence coded (DSSS) signal has similar bandwidth characteristics, which are 50 μs chip duration, 25.55 ms each (DSSS) signal duration and 80 kHz carrier frequency. The summation of seven (DSSS) signals does not have a sinusoidal shape. Its shape is similar to the noise signal except for its amplitude level. However, the frequency domain characteristic of this summation signal shows similarity with a DSSS signal; that the summation of seven (DSSS) signal is also a spread spectrum signal.
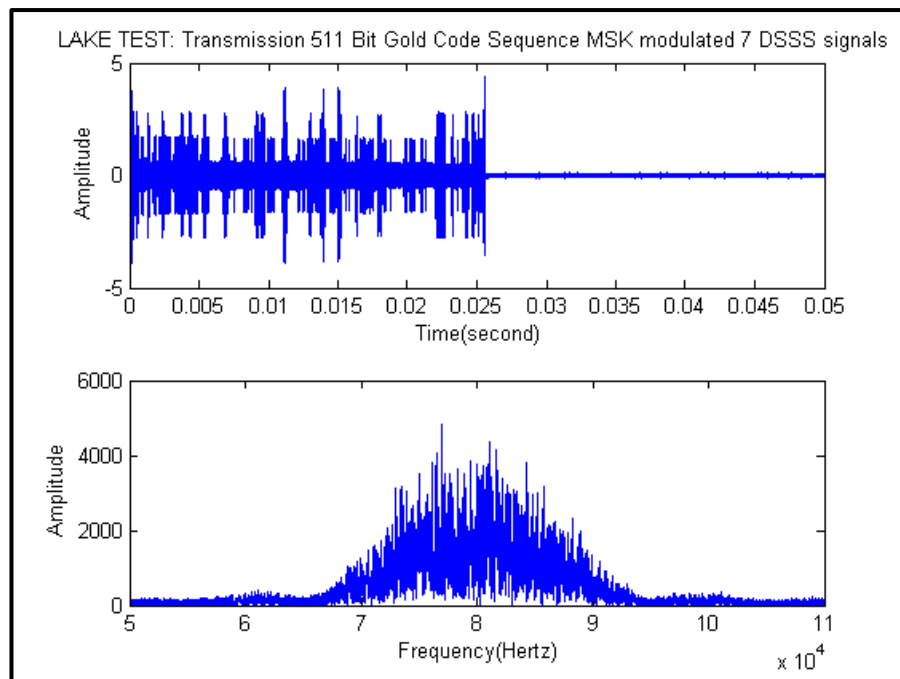

Figure 5.8: Time Domain and Frequency Domain Representations of (DSSS) Transmitted Signal

The time domain and the frequency domain representations of the received DSSS signal are plotted in Figure 5.9. The time domain representation of the received signal shows the noise signal characteristic more than the transmitted signal due to environmental noise and reverberation. The frequency domain representation of received signal shows that more signal energy is relatively scattered out of the spreading band. As a result of this, maximum point levels of the matched filters decrease.
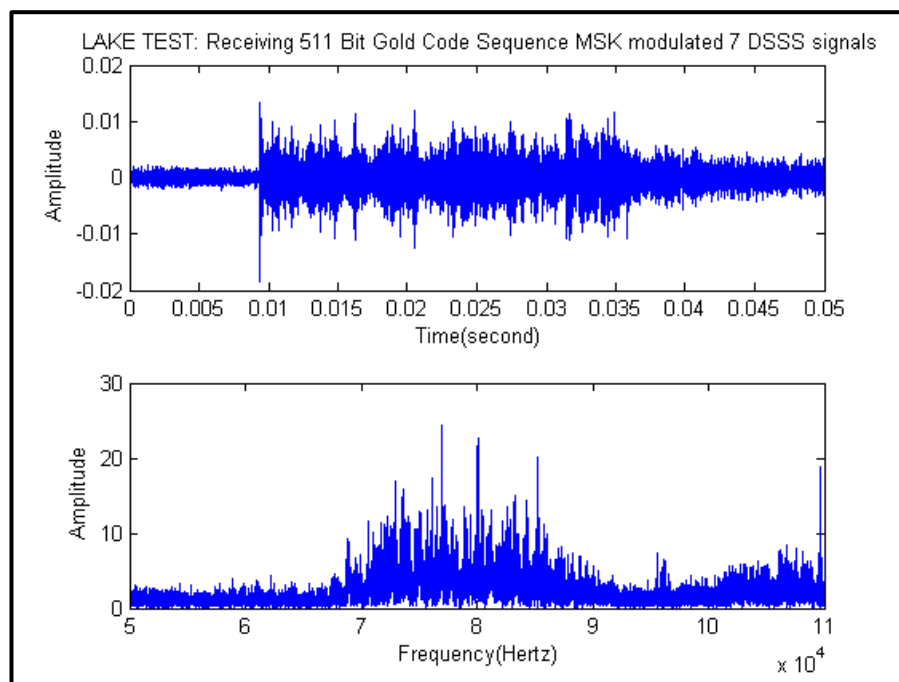

Figure 5.9: Time Domain and Frequency Domain Representations of (DSSS) Received Signal

Since the transmitted (DSSS) signal includes seven different (DSSS) code sequences, each code sequence can be separately detected by using different matched filters. Thus, each code sequence has to have its own matched filter. These matched filter output results are plotted in Figure 5.10, Figure 5.11, Figure 5.12, Figure 5.13, Figure 5.14 and Figure 5.15 for each code separately. Matched filter outputs have only one peak that is the direct path of the transmitted (DSSS) signal. As opposed to the matched filter outputs in the first step of the experiment,

the multi-path of the transmitted (DSSS) signals are not detectable due to the high distortion on the multi-path signals.

According to the matched filter output figures, maximum points of matched filter outputs are approximately at 9.37 ms with an estimated range of 14.055 meters by assumption of 1500 m/s sound velocity. According to each matched filter output result, each (DSSS) code can detect a target individually and the detection parameter of each code is as follows:

1. Code 1 detection is at 9.36 ms, in which the matched filter level is 124.3 units.

2. Code 2 detection is at 9.356 ms, in which the matched filter level is 115.8 units.

3. Code 4 detection is at 9.37 ms, in which the matched filter level is 109.2 units.

4. Code 5 detection is at 9.369 ms, in which the matched filter level is 109.9 units.

5. Code 6 detection is at 9.356 ms, in which the matched filter level is 112.2 units.

6. Code 7 detection is at 9.37 ms, in which the matched filter level is 111 units.

The maximum points of all matched filter outputs are approximately equal to each other. However, these maximum point levels are lower than the maximum point level of the matched filter (Figure 5.7) in the first step of the experiment. It means that beam coding by applying the summation of seven (DSSS) signal results in detection performance reduction on the receiver. On the other hand, these results indicate that beam coding is technically feasible for underwater acoustic systems.
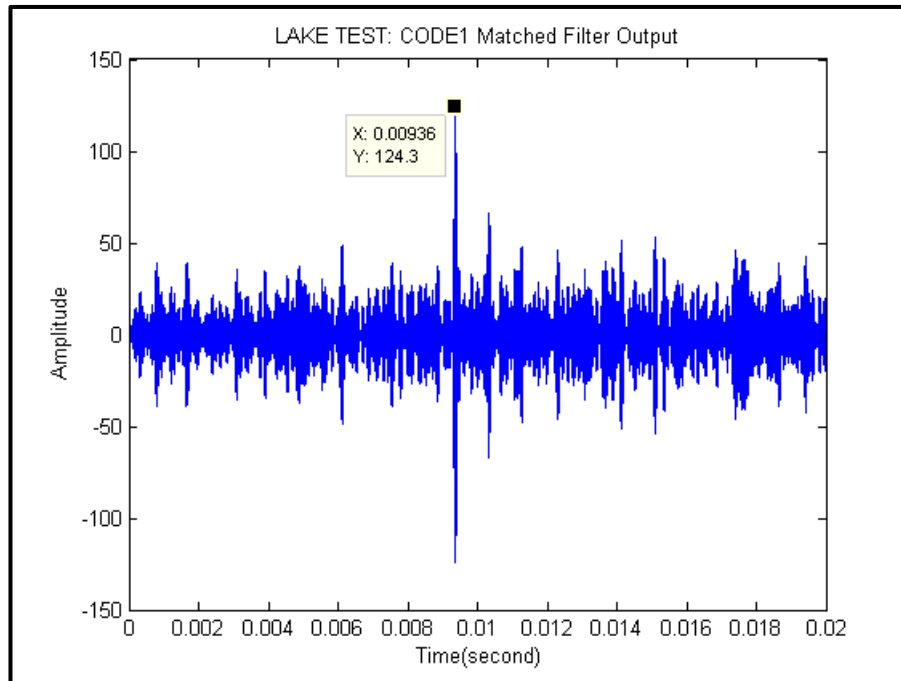
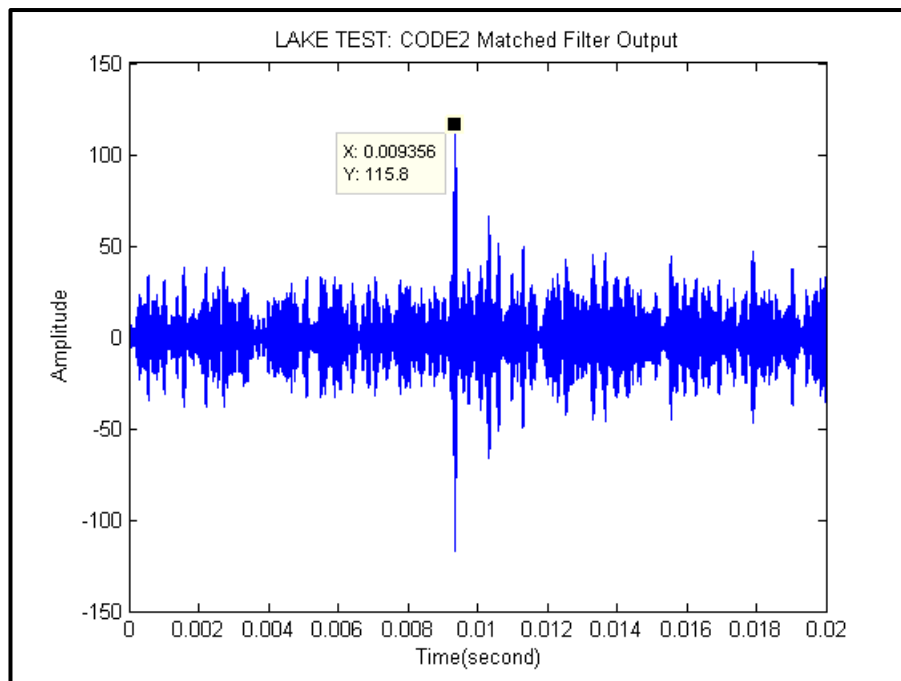Figure 5.10: 1. Coded Beam: CODE1 Matched Filter Output

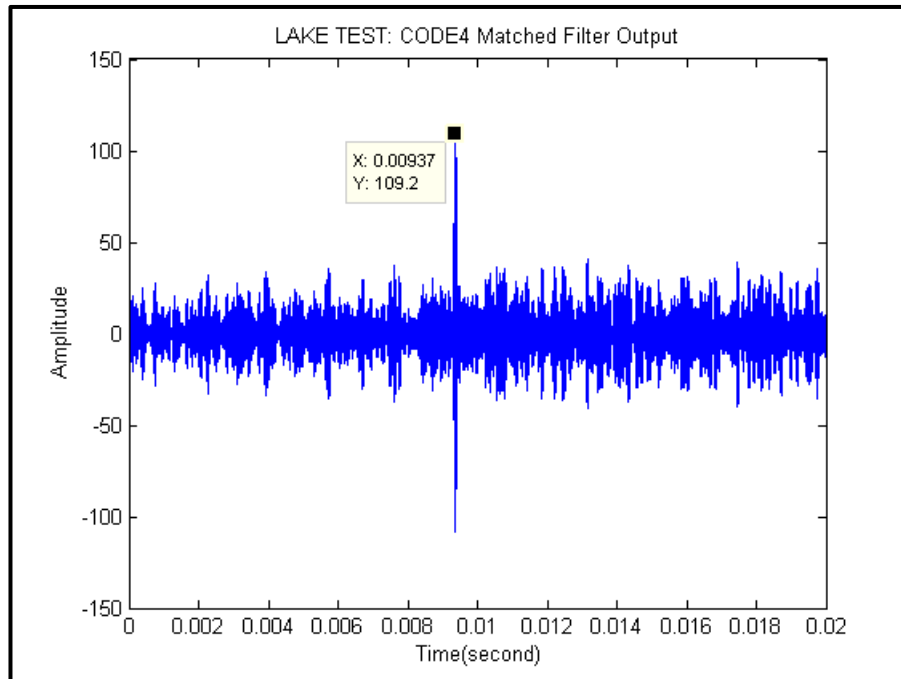Figure 5.11: 2. Coded Beam: CODE2 Matched Filter Output

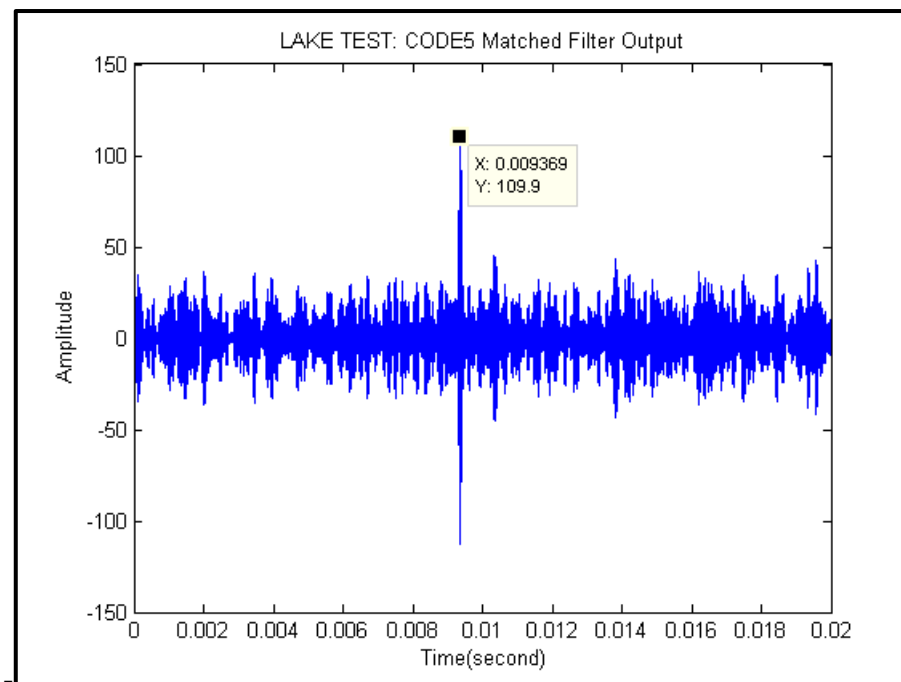Figure 5.12: 4. Coded Beam: CODE4 Matched Filter Output

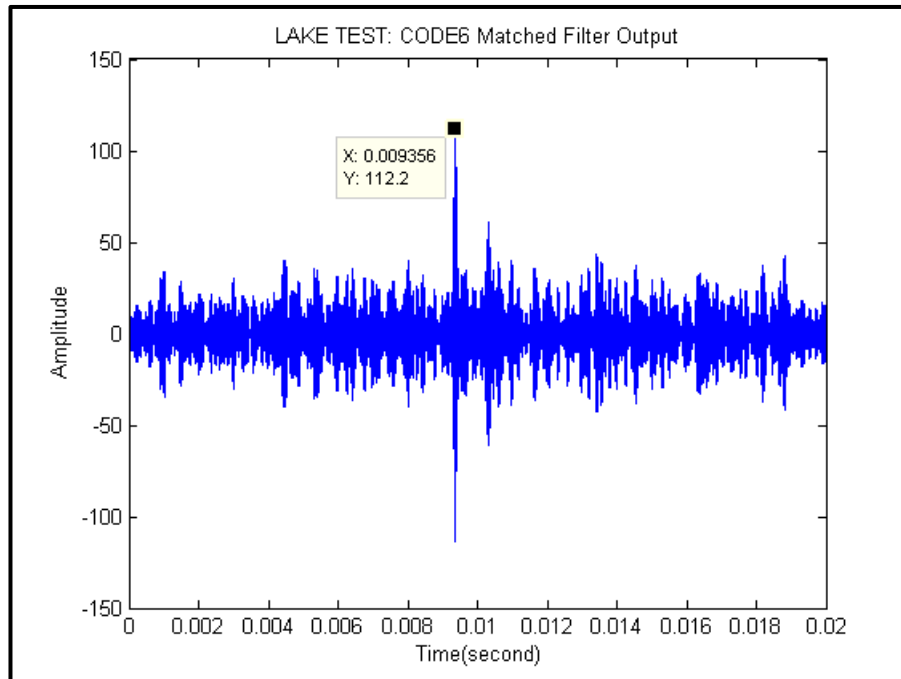Figure 5.13: 5. Coded Beam: CODE5 Matched Filter Output

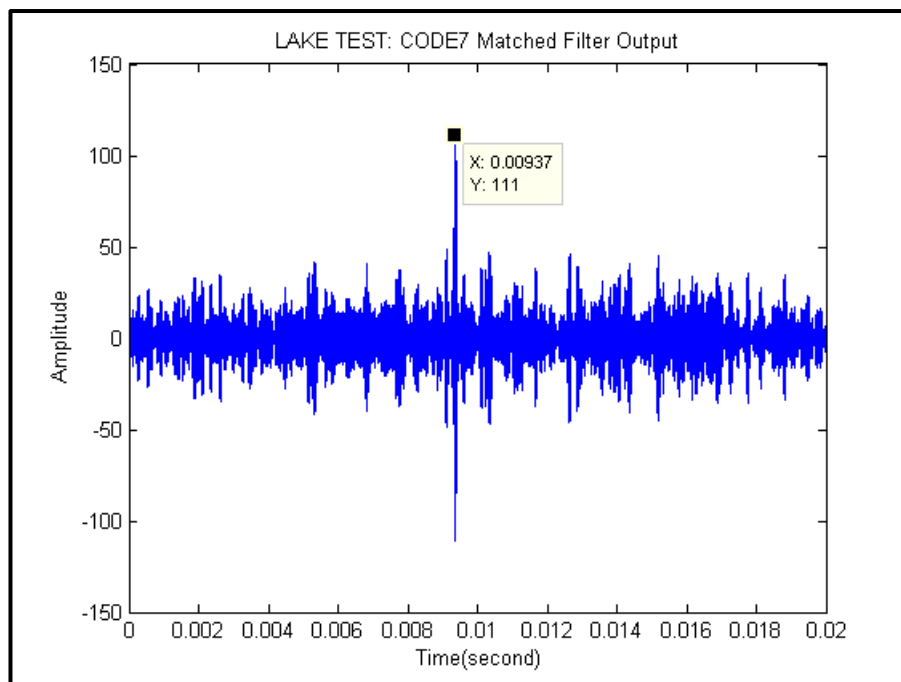Figure 5.14: 6. Coded Beam: CODE6 Matched Filter Output

Figure 5.15: 7. Coded Beam: CODE7 Matched Filter Output

5.5 The Experimental Discussion and Comparison

(DSSS) signals used in the experiments are generated by using 511 chips gold code sequence with (MSK) modulation. The experimental results indicate that (DSSS) signals with these parameters are appropriate for the beam coding approach in underwater acoustic systems.

Also, the experiments compare the (MSK) and (BPSK) modulation techniques in order to prove the performance of the (MSK) modulation with respect to the conventional (DSSS) modulation technique (BPSK). In the experiments, (BPSK) modulated (DSSS) signals that have similar parameters with the (MSK) modulated (DSSS) signal is also applied. The (BPSK) modulated (DSSS) signals also consist of 511 chips gold code sequence, where each chip has duration of 50 μs in the sequence. The result of that transmitted (DSSS) signal total duration is also 25.55 ms. The carrier frequency of gold code sequence is also 80 kHz.

Both the matched filter performance and the interference performance of (BPSK) modulated (DSSS) signals are compared to the (MSK) modulated and (DSSS) signals. The matched filter performance can be measured by comparing the maximum point of the matched filter outputs. The interference performance can be measured by comparing the maximum point of the 511 chips gold code sequence and matched filter outputs.

The matched filter performance comparison between the (BPSK) modulated (DSSS) signals and the (MSK) modulated (DSSS) signals are illustrated in Figure 5.16. The red plot is the matched filter output of the BPSK modulated (DSSS) signal and the blue plot is the (MSK) modulated (DSSS) signal. Even if the maximum points of matched filter outputs are at different times, time difference is negligibly small. The matched filter output of the maximum point of the (MSK) modulated (DSSS) signal is 822.2 units. The matched filter output maximum point of the (BPSK) modulated (DSSS) signal is 745.7 units.

This means that the (MSK) modulated (DSSS) signal provides better processing gain than the (BPSK) modulated (DSSS) signal.
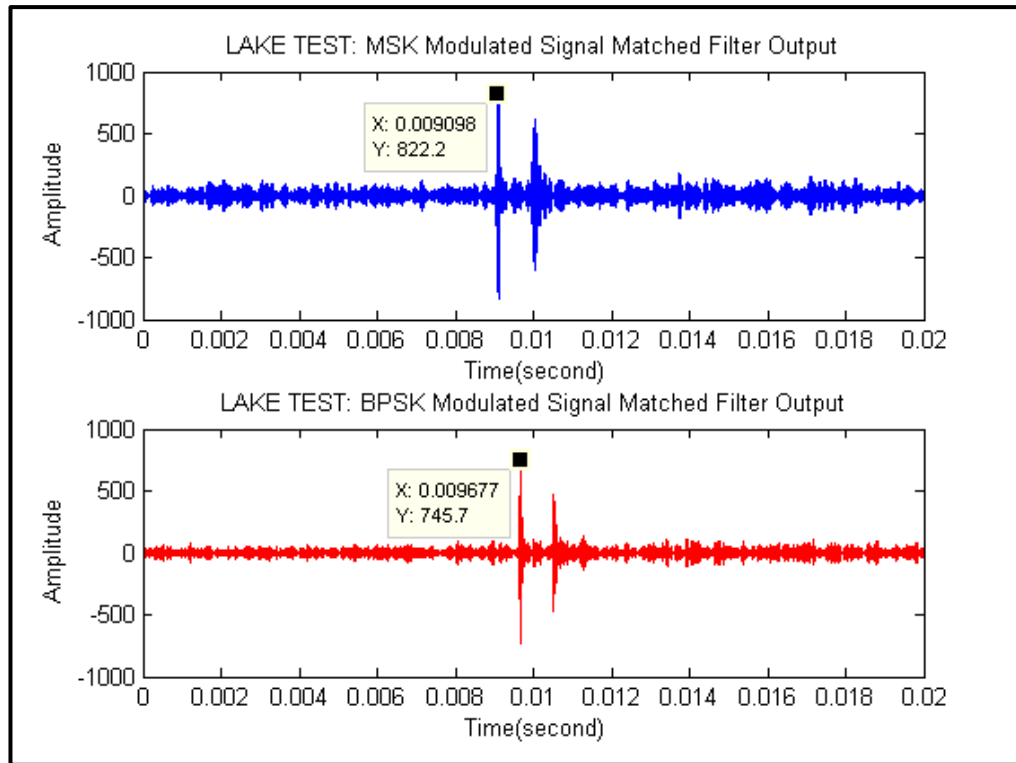

Figure 5.16: Comparison of (BPSK) and (MSK) Modulation Matched Filter Output

Interference performance comparison between the (BPSK) modulated (DSSS) signals and the (MSK) modulated (DSSS) signals are illustrated in Figure 5.17, Figure 5.18, Figure 5.19, Figure 5.20, Figure 5.21 and Figure 5.22 for each code separately. The red plots are the matched filter output of the BPSK modulated (DSSS) signal, while the blue plots are the (MSK) modulated (DSSS) signal. Due to the fact that the (DSSS) transmitted signal includes seven different (DSSS) code sequences, each code sequence has its own matched filter output results.

According to the matched filter output figures, the maximum points of (BPSK) modulated (DSSS) signals matched filter outputs are approximately at

9.249 ms whose estimated range is 13.8735 meters with an estimated velocity of 1500 m/s sound. The maximum points of the (MSK) modulated (DSSS) signals matched filter outputs are approximately at 9.37 ms, whose estimated range is 14.055 meters with assumption of 1500 m/s sound velocity. Both the (MSK) and (BPSK) modulated (DSSS) signals can detect targets individually. According to each matched filter output result, the matched filter output maximum point of each code in both the (MSK) and (BPSK) modulated (DSSS) signals are as follows:

1. Code1 (BPSK) modulated (DSSS) signal matched filter maximum point is 106.2 units. Code1 (MSK) modulated (DSSS) signal matched filter maximum point is 124.3 units.

2. Code2 (BPSK) modulated (DSSS) signal matched filter maximum point is 111.5 units. Code2 (MSK) modulated (DSSS) signal matched filter maximum point is 115.8 units.

3. Code4 (BPSK) modulated (DSSS) signal matched filter maximum point is 105.9 units. Code4 (MSK) modulated (DSSS) signal matched filter maximum point is 109.2 units.

4. Code5 (BPSK) modulated (DSSS) signal matched filter maximum point is 101 units. Code5 (MSK) modulated (DSSS) signal matched filter maximum point is 110.6 units.

5. Code6 (BPSK) modulated (DSSS) signal matched filter maximum point is 109.7 units. Code6 (MSK) modulated (DSSS) signal matched filter maximum point is 112.2 units.

6. Code7 (BPSK) modulated (DSSS) signal matched filter maximum point is 113 units. Code7 (MSK) modulated (DSSS) signal matched filter maximum point is 111 units.
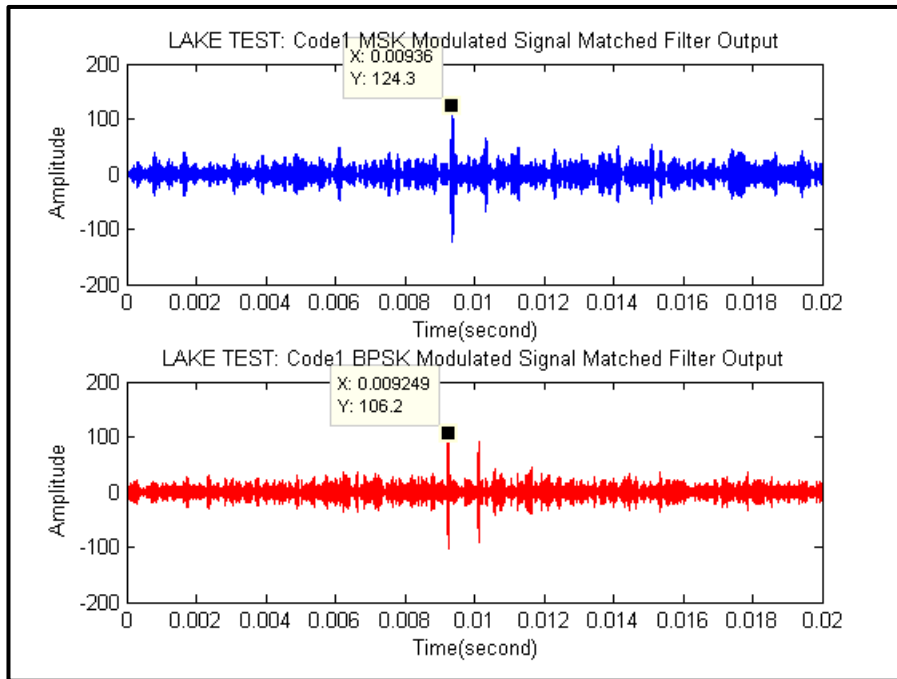
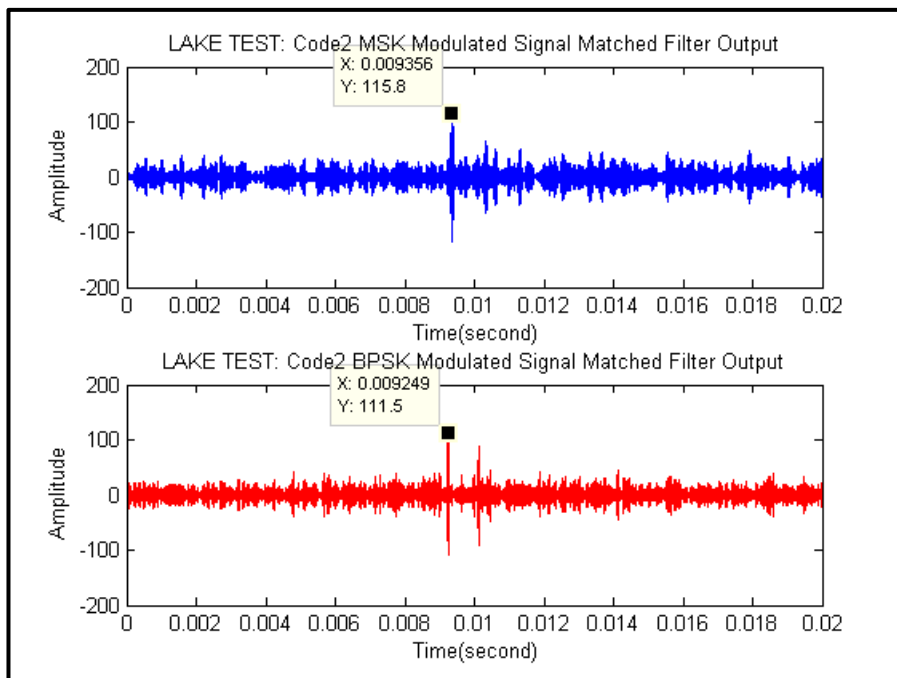Figure 5.17: 1. Coded Beam: CODE1 Comparison of (BPSK) and (MSK)
Modulation

Figure 5.18: 2. Coded Beam: CODE2 Comparison of (BPSK) and (MSK)
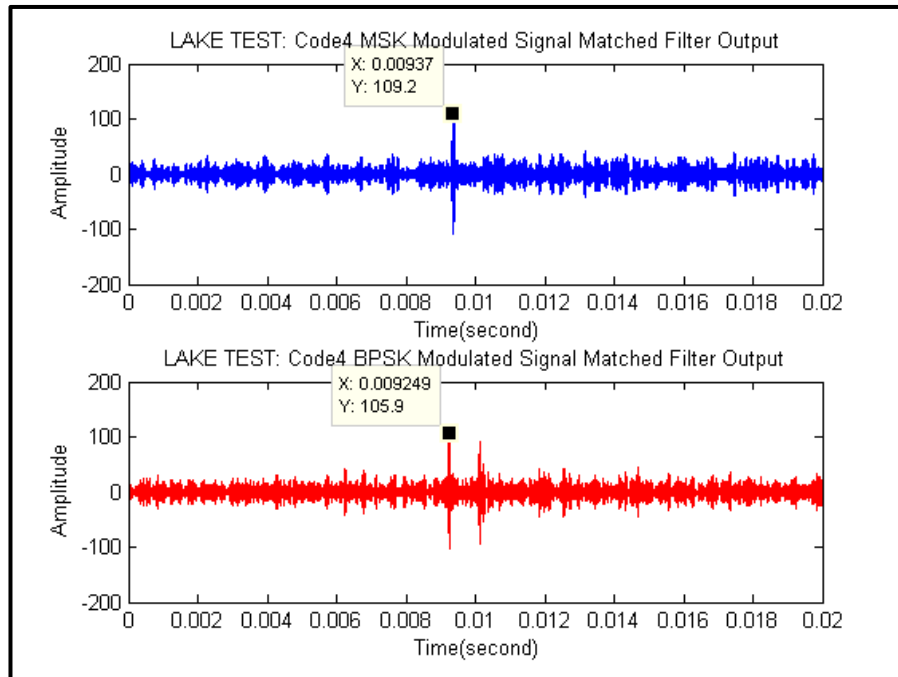Modulation

Figure 5.19: 4. Coded Beam: CODE4 Comparison of (BPSK) and (MSK)
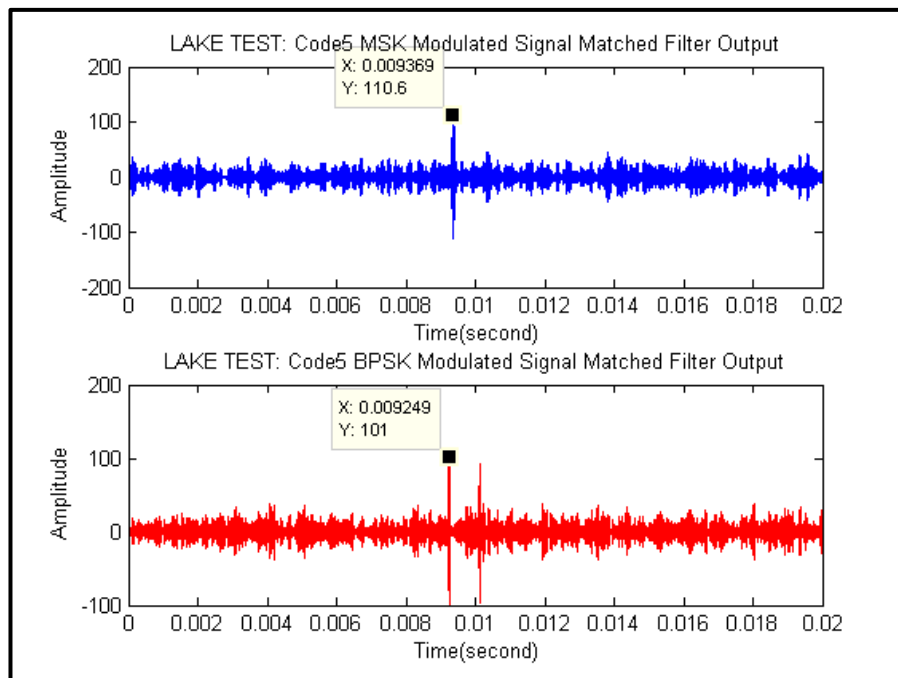Modulation

Figure 5.20: 5. Coded Beam: CODE5 Comparison of (BPSK) and (MSK)
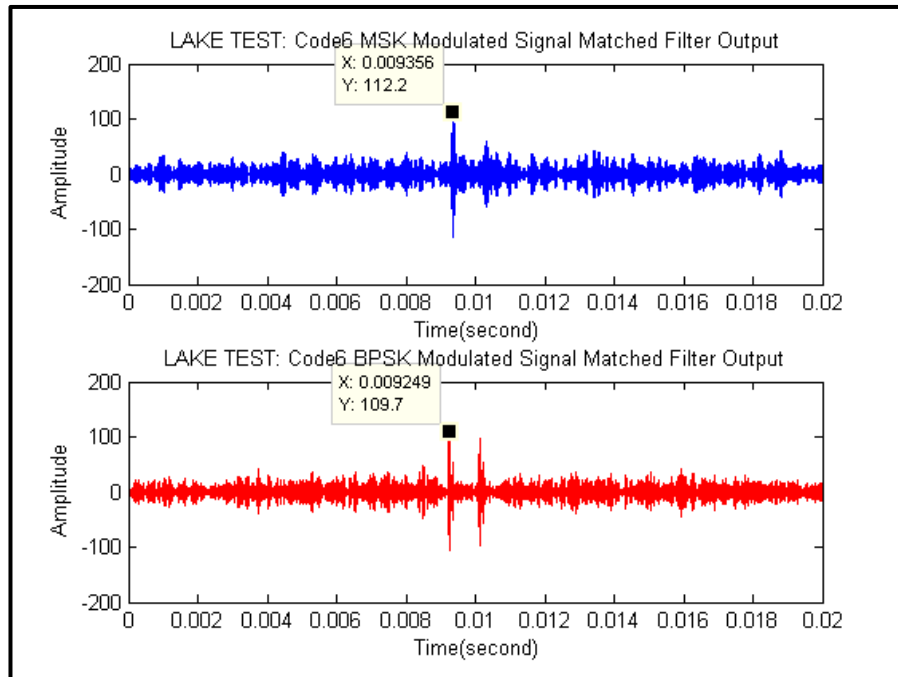Modulation

Figure 5.21: 6. Coded Beam: CODE6 Comparison of (BPSK) and (MSK)
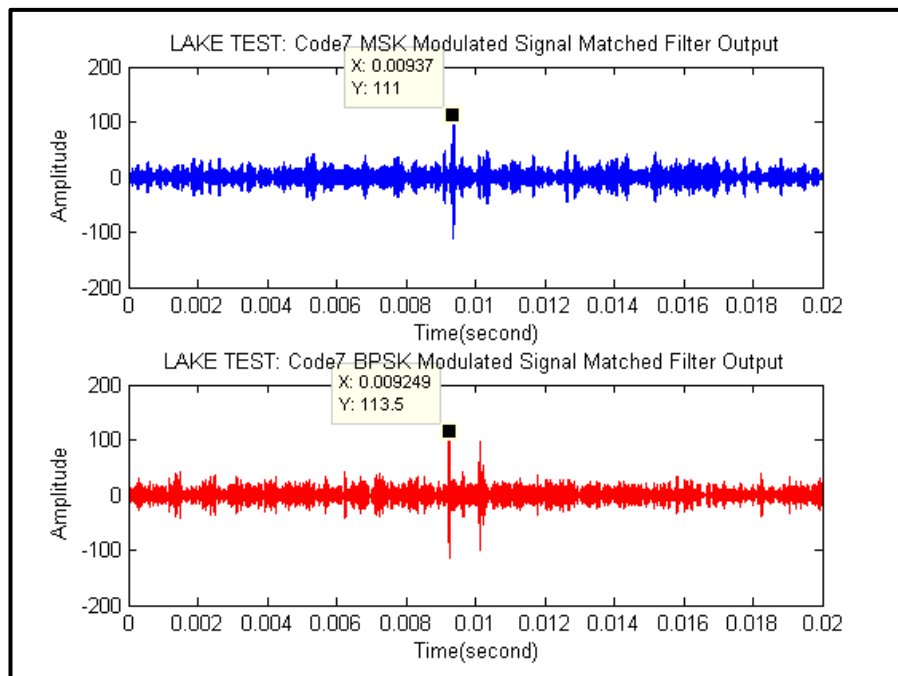
Modulation

Figure 5.22: 7. Coded Beam: CODE7 Comparison of (BPSK) and (MSK)

Modulation

The maximum point of the (MSK) modulated (DSSS) signals matched filter outputs are generally higher than the (BPSK) modulated (DSSS) signals. Only code7 provides better interference performance with (BPSK) modulation. The result of this is that the (MSK) modulated (DSSS) signals provide better processing gain and interference performance than the (BPSK) modulated (DSSS) signals except for code7.

Chapter 6

6. CONCLUSION

The term "beam coding" comes from the words "beam" and "code" and means the transmission of distinct coded signals to distinct beams. The beam is totally related with the electro acoustic antenna structure and coding is totally related with the modulation type of the acoustic signal. The main motivation of beam coding is multiple target detection at a larger surveillance area without loss of beam resolution by the help of coded signals.

The applicability of beam coding in underwater acoustic systems was the focus of this study. For this purpose, direct sequence spread spectrum (DSSS) coded signals were used. The performance of (DSSS) coded signals was investigated for beam coding application. Gold code sequences that have better cross-correlation properties were used for coded signals instead of the well-known maximal-length code sequence. Also, a minimum shift keying (MSK) modulation that provides phase continuity of coded signal was used in order to modulate code sequences instead of the widely used binary phase shift keying modulation (BPSK).

There are two significant elements in the design of coded (DSSS) signals and these are the selection of pseudorandom (PN) code sequences and the conservation of signal energy within the operational bandwidth. The critical property for the selection of (PN) code sequences is orthogonality of code sequences. Generally, it is the maximal length code sequences that are used for (DSSS) signal designs in literature. However, these sequences are more suitable for single-user applications thanks to their poor cross-correlation properties. Therefore, gold code sequences that are more suitable for beam coding application are preferred thanks to their good cross-correlation properties.

For the conservation of signal energy within operational bandwidth, the critical property is phase continuity in transition from binary code '1' to '0' and vice versa. At transition points, the energy of the signal is scattered to the whole band due to the phase discontinuity. In order to avoid phase discontinuity at transition points, the (MSK) modulation, which is a special case of continuous phase frequency shift keying (CPFSK) modulation, is used for beam coding experiments.

The orthogonality of (PN) code sequences is directly proportional to their length. In order to avoid the disadvantages of long signal, the optimum length of (PN) code sequence for the METU Yalıncak Lake underwater environment was investigated. The length of the PN code sequence was determined as 511 chips for beam coding experiments.

After determining the design parameters of the coded DSSS signals, conceptual beam coding experiments were carried out in METU Yalıncak Lake in two distinct steps: the detection performance measurement of one coded (DSSS) signal and the interference performance measurement of seven coded (DSSS) signals. For the detection performance measurement of one coded (DSSS) signal, the received (DSSS) signal was passed from the matched filter and the maximum point of the matched filter output was observed with respect to the noise level of the received signal. As expected, the maximum point of the matched filter output corresponded to a distance of target (hydrophone) which was at 12.525

meters by an estimated velocity of 1500 m/s sound. Also, the multi-path of signal reflected from a surface was detected at 9.4 ms with an estimated range of 14.1 meters. This multi-path distance was verified by geometric calculations under the assumption of constant sound velocity profile. For interference performance measurement of seven coded (DSSS) signals, the summation of seven (DSSS) signals was transmitted and the received signal was passed through six different matched filters that were matched with the related coded (DSSS) signals. As expected, the maximum point of the matched filter outputs corresponded to a distance of hydrophone approximately at 14.055 meters by an estimated velocity of 1500 m/s sound. However, the maximum point level of the matched filter outputs was approximately one of seven, with respect to the maximum point level of the matched filter output at the first step of the experiment. As a result, each coded (DSSS) could be detected under some interference, which indicates that multiple target detection is possible with beam coding.

The design of (PN) code sequences plays a crucial role for beam coding application and almost an infinitive combination of (PN) code sequences is possible. Since the main motivation of this study is beam coding, (PN) code sequence investigation was ended after discovering the gold code sequences that are sufficiently good for beam coding. Hence, orthogonal (PN) code sequence designs can be investigated in depth in future studies. Also, other continuous phase modulation techniques can be researched for (DSSS) signals so as to prevent loss of signal energy. Experiments that are conducted in this study are conceptual proof of beam coding applicability in underwater acoustic systems. This conceptual proof can be experimentally proved by conducting additional experiments that are related to the transmission of each coded (DSSS) signal to different angles by using beam steering electronically.

Bibliography

[1] D T. Blackstock, "Fundamentals of Physical Acoustic", A-Wiley interscience publication, 2000, pp. 1-4

[2] C. H. Sherman and J. L. Butler, "Transducers and Arrays for Underwater Sound". Springer, 2006, pp. 1-9

[3] M.O. Güleryüz, Low power range estimation with DSSS technique in underwater acoustics. Bilkent University, M.Sc. Thesis, August, 2013.

[4] Y. Kumru, "Using Spread Spectrum Coded Pings in Active Sonar Technology" Bilkent University, M.Sc. Thesis, July, 2014.

[5] P. M. Cassereau and J. S. Jaffre " Frequency Hopping Pattern for Simultaneous Multiple-Beam Sonar Imaging" Woods Hole Oceanographic Institution Department of Ocean Engineering Woods Hole, Massachusetts 02543

[6] J. S. Jaffre, P. M. Cassereau and D.J. Glassbrenner "Code Design and Performance Characterization for Code Multiplexed Imaging" IEEE Transactions on Acoustic Speech and Signal Processing Vol. 38, No.8, August 1990.

[7] J. Han, S. Kim, K. Kim, W. Choi, M. Kim, S. Chun and K. Son "A study on the underwater acoustic communication with direct sequence spread spectrum," IEEE Embedded and Ubiquitous Computing Conf. Proc. Vol. 2, 2010, pp. 337-340.

[8] Simon Haykin, "Communication Systems Fourth Edition". John Wiley & Sons, Inc., 2001,

[9] D. Prabakaran, "Spread Spectrum Technology and Its Applications" Electronics For You, December 2005, pp.104-114.

[10] R. Malik, "Spread Spectrum – Secret Military Technology to 3G" http://ethw.org/images/a/a3/SpreadSpectrum.pdf Last Accessed: 30.07.2015

[11] A. J. Viterbi, "Spread Spectrum Communications - Myths and Realities" IEEE Communications Magazine, May 1979, pp.11-18.

[12] R. J. Urick, Principles of Underwater Sound. Peninsula Publishing 3rd edition, 1983.

[13] J.G. Proakis and M. Salehi. "Digital Communications" Fifth Edition, McGraw-Hill Higher Education, 2008.

[14] V. K. Garg, "Wireless Network Evolution 2G to 3G". Prentice Hall PTR, 2001.

[15] R. L. Peterson, R.r E. Ziemer and D. E. Borth, "Introduction to Spread Spectrum Communicaitons", Prentice-Hall Inc. 1995.

[16] W. W. Peterson and E. J. Weldon, "Error Correction Codes" (Cambridge: MIT Press, 1972)

[17] K. Metzger and R. J. Bouwens, "An Ordered Table of Primitive Polynomials over GF(2) of degrees 2 Through 19 for Use with Linear Maximal Sequence Generators ", TM107, Cooley Electronics Laboratory, University of Michigan, Ann Arbor, July 1972 .

[18] S. Haykin, and M. Moher, "Modern Wireless Communication" Pearson Prentice-Hall Inc. 1995.

[19] X. Lurton, "An Introduction to Underwater Acoustics Principles and Applications" Springer 2002. Pages: 103.

APPENDIX A

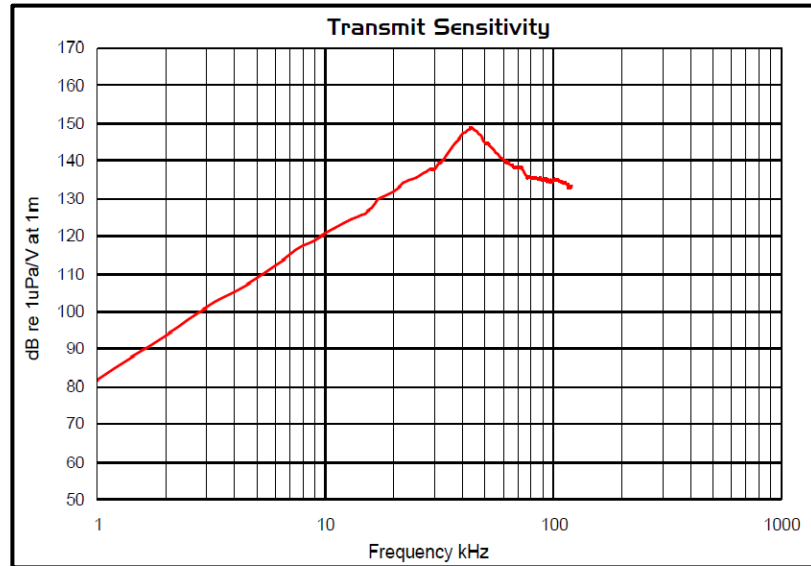**Neptune Sonar D45 Transmitting Voltage Response (TVR)**

Figure: Neptune Sonar D45 Transmitting Voltage Response (TVR) Graph

Electro acoustic antennas are linear devices that transform electricity into acoustic pressure or vice versa. The response of transducers is called transmitting voltage response (TVR). The TVR of transducers is generally measured in the maximum transmission direction with the reference voltage (1V), the reference acoustic pressure (1μPa) at the reference distance (1m). The TVR of a transducer is calculated as follows:

$$\text{TVR} = 20 \log_{10} \frac{P_{1v}}{P_{ref}} \qquad \text{in dB re 1μPa/ 1m/1V}$$

where P_{ref} is the reference acoustic pressure and P_{1v} is the acoustic pressure at 1m away from the transducer.

The Neptune Sonar D45, whose TVR graph can be found above, was used as the transducer in the lake experiments. The TVR of this transducer is approximately 135 dB at our operational bandwidth (70 – 90 kHz) of this study.

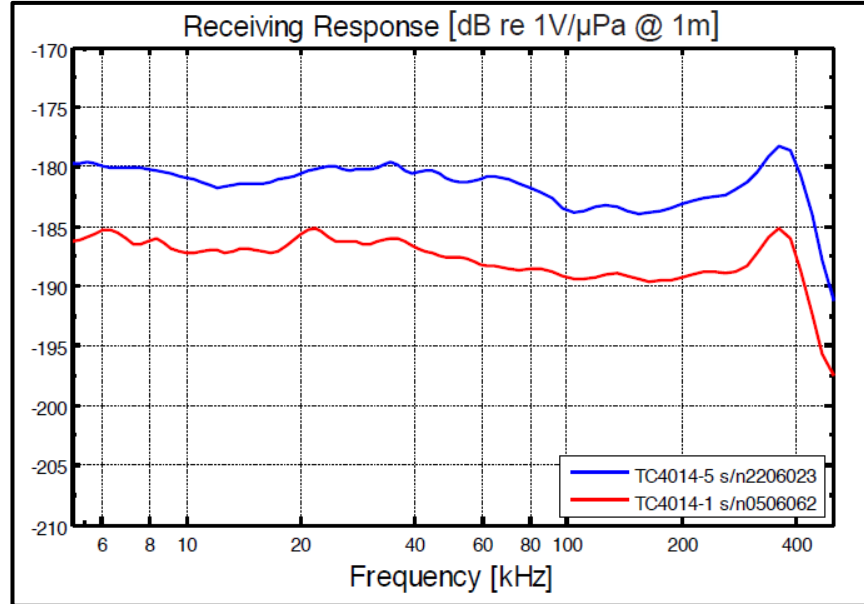**Teledyne Reson TC4014-5 Receiving Sensitivity**

Figure: Teledyne Reson TC4014-5 Receiving Sensitivity Graph

Electro acoustic antennas are linear devices that transform electricity into acoustic pressure or vice versa. The response of hydrophone is called receiving sensitivity. The receiving sensitivity of hydrophones is generally measured in the maximum reception direction with the reference voltage (1V), the reference incident acoustic pressure (1μPa). The receiving sensitivity of a hydrophone is calculated as follows:

$$\text{TVR} = 20 \log_{10} \frac{V_{1\mu Pa}}{V_{ref}} \qquad \text{in dB re 1V/ 1μPa}$$

where V_{ref} is the reference voltage and $V_{1\mu Pa}$ is the electric voltage of hydrophone.

The Teledyne Reson TC4014-5, whose receiving sensitivity graph is shown above, was used as the hydrophone in the lake experiments. Receiving sensitivity of this hydrophone is approximately -182 dB at our operational bandwidth (70 – 90 kHz) of this study.